2014

Mixed Mode (I-Ii) Delamination Fracture Criteria For Im7-G/8552 Intermediate Modulus Carbon/Epoxy Composite Laminate

Jr. Samuel Williams
North Carolina Agricultural and Technical State University

Mixed Mode (I-II) Delamination Fracture Criteria for IM7-G/8552 Intermediate Modulus Carbon/Epoxy Composite Laminate

Samuel Laverne Williams, Jr.

North Carolina A&T State University

A thesis submitted to the graduate faculty

in partial fulfillment of the requirements for the degree of

MASTER OF SCIENCE

Department: Mechanical Engineering

Major: Mechanical Engineering

Major Professor: Dr. Kunigal Shivakumar

Greensboro, North Carolina

2014

The Graduate School
North Carolina Agricultural and Technical State University
This is to certify that the Master's Thesis of

Samuel Laverne Williams, Jr.

has met the thesis requirements of
North Carolina Agricultural and Technical State University

Greensboro, North Carolina
2014

Approved by:

Dr. Kunigal Shivakumar Major Professor	Dr. Raghu Panduranga Committee Member
Dr. Robert Haynes Committee Member	Trisha Sain Committee Member
Dr. Samuel Owusu-Ofori Department Chair	Dr. Sanjiv Sarin Dean, The Graduate School

Biographical Sketch

Samuel L. Williams, Jr., earned his Bachelor of Science degree in Mechanical Engineering from North Carolina Agricultural and Technical State University in 2012. His hometown is located in Detroit, MI. He grew up in a military household, his dad, Chief Petty Officer Samuel L. Williams, Sr., proudly served 33 years in the United States Navy. His Mother, Dr. Wanda Jackson, is a NASA particle physicist and university professor. Samuel's yearning for knowledge, pursuit of a higher education and the unwavering discipline to complete his goals all stemmed from his upbringing. He is currently a candidate for the Masters of Science degree in Mechanical Engineering. Samuel's lifelong goals include pioneering the next generation of space vehicles and serving his country as an officer in the United States Navy.

Dedication

I dedicate this Master's Thesis to my beloved family and friends, Dr. Wanda G Woodson-Jackson, Alexis Camoille Woodson-Jackson, Valerie Brooks and Samuel L. Williams, Sr., for their love, and continuous support. I, mostly humbly, dedicate this thesis to my lord and Savior, for through his love, protection and favor, all things are possible.

Acknowledgements

I would like share acknowledgement to my advisor, Dr. Kunigal Shivakumar for the guidance and support during challenging times in the course of the research. I wish to express my appreciation to my thesis committee members, Dr. Raghu Panduranga, Dr. Trisha Sain, and Dr. Robert Haynes for their time to review and offer constructive criticism of my thesis. I acknowledge the financial support of NASA Grant (NNX09AV08A) and VLRCOE contract #W911W6-11-2-0012.

I thank the staff and faculty of Center of Composite Material Research, Center of Aviation Safety (CAS), and Department of Mechanical Engineering for their support during my research, especially, Mr. Matthew Sharpe, Laboratory Manager, Mr. John Skujins, for their assistance in completing this work.

I must also acknowledge former and current students of CCMR: Rafid Kully, Hiba Ahmed, Kazi Inman, Sidharth Karnati Reddy and ARL researchers: Dr. Asha Hall, Dr. Jaret Riddick and Michael Coatney who provided their expertise, advice and assistance to the culmination of this thesis.

Table of Contents

List of Figures

List of Tables

Abstract

In aerospace vehicles such as rotorcraft, structural components are subjected to bending and stretching loads that introduce peel and shear stress between the composite plies. Delamination is a primary failure mode for composite laminate. Delamination is caused by interlaminar stresses that act in the matrix, which is the weaker part of the composite laminate. Damage tolerant design of structures requires two types of material/laminate data: 1. Mixed mode delamination criteria to predict failure and 2. Delamination growth criteria to predict the life of a structural component. This research focuses on developing mixed-mode (a combination of mode I and II) fracture criteria for IM7-G/8552 composites, which are widely used in the rotorcraft industry. IM7-G/8552 prepreg was procured from the HEXCEL Corporation and 24 ply unidirectional laminate with a 3 in width Fluorinated ethylene propylene film was fabricated. Standard split beam specimens were prepared. The specimens were tested in double cantilever beam and end notched flexure beam modes to measure mode I (G_{IC}) and II (G_{IIC}) fracture toughness, respectively. Split beam specimens were tested using the modified mixed-mode test apparatus for values of GIIm/GC = 0.18, 0.37, 0.57 and 0.78, where G_C is the total fracture at GIm and GIIm loading. From the data, a mixed mode fracture equation was developed in the form:

$$G = G_{IC} + 115\left(\frac{G_{II}}{G_c}\right) + 550\left(\frac{G_{II}}{G_c}\right)^2$$

The equation agreed well with the literature for G_{IC}, and $G_{II}^m/G_C = 0.33$ but it differs at $G_{II}^m/G_C = 0.66$ and G_{IIC}.

CHAPTER 1

Introduction

A background and the applications of Polymer Composites materials in aerospace and rotorcraft structures, and advantages, disadvantages and limitations of polymer composites are presented. A brief overview of the fracture test methods and toughness characterization for unidirectional composite laminates are described. Finally, the current objectives of the research and the scope of the thesis will be discussed.

1.1 Background

A composite material consists of two or more materials that are in combination at the microscopic scale to form a new, improved and invaluable material than its components. The two main parts of a composite are the matrix and reinforcement. The matrix is essentially a binder that encompasses the reinforcement and helps maintain its relative positions. The reinforcement material provides the mechanical strength and stiffness to the composites. Together, forms an effective composite. A synergism produces material properties that are superior to the individual components. A variety of matrix and reinforcements allows the product designer to select the most efficient material combination for the chosen application.

Fiber reinforced composites are classified into certain categories according to form of reinforcement and type of matrix material used. Based on the type of reinforcements used, composite materials are classified into two main categories [Daniel & Ishai, 2005]. Discontinuous and continuous fiber reinforced composite materials as shown in figure 1.1. Discontinuous fibers that make up a composite are essentially, particles, flakes, chips, short fibers or etc., that are stacked together in a certain layout in order to produce a laminate. Continuous fiber reinforced composite materials have a certain orientational axes which makes

them ideal for certain applications. They could be unidirectional, cross ply, or multidirectional. Reinforcement materials are commercially made and available in a variety of forms. The forms are not limited to unidirectional tapes, plain weave, harness satins, breaded and stitched.

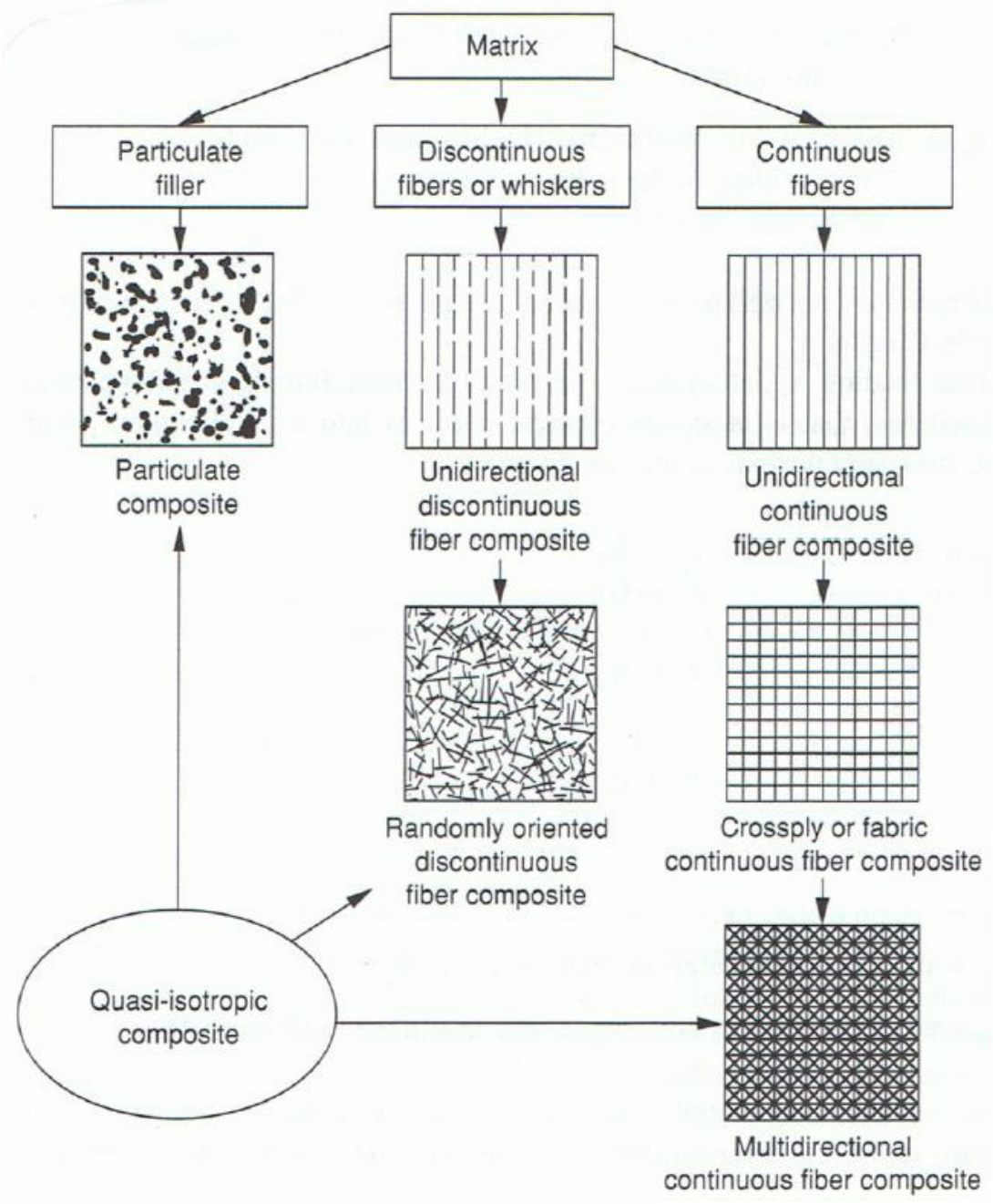

Figure 1.1: Classification of Composite material system (Daniel & Ishai, 2005).

In addition to Composite classification of composites is based on fibers, they can also be identified by the type of matrix used. Subsequently, they are classified as PMC (Polymer matrix composites), MMC (Metal Matrix Composites), and CMC (Ceramic Matrix Composites). Polymer Matrix Composites are comprised of thermosetting (epoxy, polyamide, polyester) or thermoplastic (polysulfone, poly-ether-ketone) resins. These materials are reinforced with either glass, carbon (graphite), aramid (Kevlar) or boron fiber. Metal Matrix Composites incorporate metal materials for its matrix such as aluminum, magnesium, titanium, or copper) reinforced with boron, carbon (graphite), or ceramic fibers. The primary limitation of the MMC is the softening or melting temperature of the metal matrix. CMCs encompass ceramic matrices such as silicon carbide, aluminum oxide, glass ceramic, or silicon nitride. These matrices are reinforced with ceramic fibers.

Laminated Composites are made up of two or more unidirectional or multidirectional plies which are stacked and cured together. These plies are placed in various orientations to allow for the maximum strength within the material axes. Figure 1.2 illustrates the various orientations. The orientation of a given ply is provided by the angle between the reference x-axis and the major principal material axis of the ply, measured in a counterclockwise direction on the x-y plane (Daniel & Ishai, 2005).

The fabrication process of composite laminates consists of several steps which include cutting the prepreg plies, stacking into desired orientation, debulking, and molding in an autoclave process. The extreme heat and pressure from the autoclave produces a composite laminate of higher strength and improved material properties. Composite laminates present the opportunity to design specialized and application specific material in one unified and synchronous process. In the automotive and infrastructure industries, the high volume

application will increase the usage of PMC's (polymer matrix composites) tremendously. There are certain deficiencies of the laminated composites. These drawbacks include but are not limited to, the high cost of tooling, machining and assembly. In addition to the mentioned setbacks, the real-time and severe problems of delamination between the adjacent layers within the laminated composite are of much concern to the scientific community.

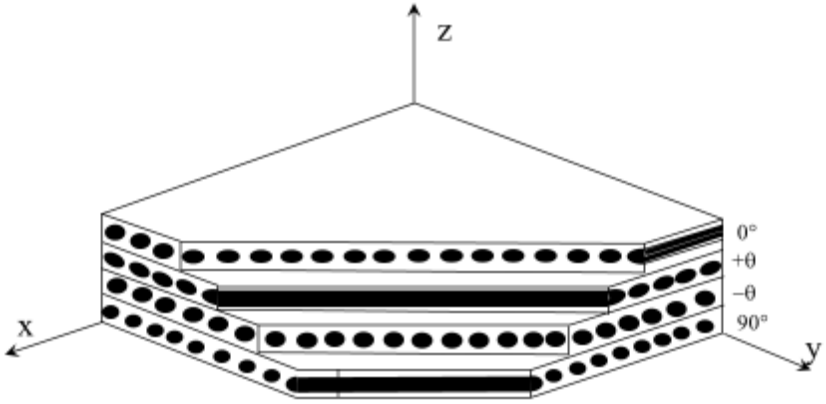

Figure 1.2: Multidirectional laminate and reference coordinate system (Daniel & Ishai, 2005).

1.1.1 Advantages of Composite Laminates

Composites have unique advantages over the metallic materials used today. These advantages are higher strength, high stiffness, longer fatigue life, lower density, corrosion resistance and shapability to fit various structures and/or components. Additionally, there are benefits that include acoustic insulation, increased wear resistance and improved thermal insulation. The foundation for the composites superior structural performance relies heavily on its high specific strength and high specific stiffness of the material. Its high specific strength stems from the materials strength-to-density ratio and the high specific stiffness stems from the materials modulus-to-density ratio. By selecting the appropriate combination of reinforcement and matrix materials, manufacturers have the ability to design and construct a material with specified properties for whatever application they are tasked with.

1.1.2 Disadvantages of Composite Laminates

In contrast to the advantages, there are disadvantages and limitations to composite materials. These limitations are not shared by the conventional and consistent materials currently used in aerospace, automotive and infrastructure industries. The most prominent disadvantage within the composite is the susceptibility to delamination. That occurs when the Interlaminar stresses due to the dissimilarity between the anisotropic mechanical and thermal properties of the plies occurring at the free edges, joints and under out-of-plane loading. Delamination is the dominating failure mode in composite laminates (Arguelles et al, 2009). The research literature on the modes of fracture that occur within delaminated composites is discussed in the next section.

1.2 Literature on Fracture Modes of Delaminated Composites

This review covers the fracture modes of delaminated composites and all the details are discussed below.

Delamination is the most common damage mode that composite materials are susceptible to; that is, to interlaminar cracks which are prone to appear and propagate between plies under static and dynamic conditions (Arguelles, 2009). Delamination has many adverse effects on composite, which include shortening the service life of the structure and will ultimately lead to catastrophic failure of the structure. Delamination of polymer matrix composites (PMCs) has been given considerable attention in the research community, which led to the development of standardized test methods for Mode I, Mode II and Mixed Mode (I-II) Interlaminar delamination fracture characterization (Czabaj,M.)

The energy release rate per unit area of new crack surface created by each of these above modes is represented by $G_{IC,}$ G_{IIC} and G_{I-II}. Adeyemi et al., investigated the effect of

manufacturing processes (autoclave-molded, compression molding and vacuum assisted compression molding) on delamination fracture toughness (mode I, mode II and mixed mode (I-II)) of laminated woven-fabric composites ((HMF) 5322/34C). Mode I testing was conducted using the Double Cantilever Beam (DCB) test setup, Mode II testing was conducted using the End Notched Flexure (ENF) test setup and mixed mode (I-II) was conducted using the modified mixed-mode bending apparatus. G_I/G_{II} loading ratios used were 1/4, 1/1, 2/1 and 4/1. Autoclave-molded composite had the lowest fracture toughness among other manufactured composites followed by vacuum assisted compression molding and compression molding and the present trend is the same for all the composite laminates. Since the resin content in compression molding was higher than the other manufactured composites, compression molded composites had the highest delamination fracture toughness. That was followed by vacuum assisted compression molding as it underwent the same process as the Autoclave-molded composite. The authors' concluded that higher the resin content, the delamination fracture toughness will be larger.

Czabaj and Ratcliffe conducted a study on the Mode I Interlaminar fracture toughness of IM7-G/8552 unidirectional composite laminates. From the study, it was determined that by including a Teflon insert into a laminate during the layup process as a crack initiator results in an unstable fracture propagation beyond the resin rich region. The resulting effects were artificially high initiation fracture toughness values that stabilized after the unstable fracture propagation.

Arguelles and Bonhomme conducted studies on Mode I and Mode II delamination of unidirectional carbon reinforced composites. The test were performed by following the European Structural Integrity Society (ESIS) protocol and the ASTM standards for Hexcel AS4/8552 composite laminates. Hansen and O'Brien provided literature on a study dealing with the all three modes of loading (Mode I, Mode II and the combination Mixed Mode I-II). The study

discovered that IM7-G/8552 carbon/epoxy unidirectional composite laminate yield lower fracture toughness values than from the comparison material S2/8552 glass/epoxy. Although, there was significant data scatter from the test.

O'Brien et al., presented a study on the characterization of the Mode II Interlaminar fracture toughness and delamination onset and growth for IM7/8552 epoxy composite material. The ENF test protocol for Mode II fracture toughness is under review by ASTM as a potential standard test method. It is used as guidance for this test procedure. Tests were conducted using End Notched Flexure specimens. This test involved loading a beam with a midplane starter crack, introduced during fabrication, at one end. The specimen is then loaded to failure, in a three (3-) point bending apparatus and data collected during the test. The energy release rate, G_{II}, was determined using the compliance calibration relation specified in the ASTM draft standard. Equation (1.1) shows how to compute G_{II} for a specimen with a constant width, B. Equation (1.2) can also be used to calculate the G_{II}, but this equation takes into account the compliance calibration constant, m, which is calculated from the slope of the c versus a^3 plot.

$$G_{II} = \left(\frac{P^2}{2B}\right)\left(\frac{\partial C}{\partial a}\right) \tag{1.1}$$

$$G_{II} = \left(\frac{3mP^2a^2}{2B}\right) \tag{1.2}$$

Avva et al., developed a modified mixed-mode bending apparatus to measure delaminated fracture toughness and fatigue delaminated growth rates for laminated composites based on the mixed-mode bending test apparatus developed by Crews and Reeder. Also refers to

the ASTM standard, a linear and nonlinear analysis was presented. The G and G_I/G_{II} values from both analyses were compared with each other and presented that the linear G_I Eq. (1.3) and G_{II} Eq. (1.4) equations are accurate for modified mixed-mode apparatus.

$$G_I = \left(\frac{P_I^{\,2}}{BIE_{XX}} \right) \left(a^2 + \frac{2a}{\lambda} + \frac{1}{\lambda^2} + \frac{h^2 E_{XX}}{10 G_{XZ}} \right) \tag{1.3}$$

$$G_{II} = \left(\frac{3P_{II}^{\,2}}{64BIE_{xx}} \right) \left[a^2 + \frac{h^2 E_{XX}}{5G_{XZ}} \right] \tag{1.4}$$

Mode I, Mode II and mixed mode (I-II) fracture test was conducted on 24 ply unidirectional IM7/5260 Graphite/Bismaleimide composite. DCB test specimen is used for mode I and ENF test specimen was used for mode II and modified mixed-mode bending apparatus was used for mixed mode (I-II). The results demonstrated that the delamination fracture criteria gave a lower bound solution as in many of the thermoset composites and G_R resistance was nearly constant and there was a decrease in G_I/G_{II} ratio with a delamination growth but it is small enough that it can be assumed as constant. Recently, a fracture criterion was developed with the same apparatus for AS4/8552. [Karnati, 2014]

The studies presented heretofore treated G_I and G_{II} interaction differently and have not presented the feasibility of developing a mixed Mode (I-II) fracture criteria that can be used in damage tolerant design of laminated composite structural components. The presented research is to provide a step by step approach to develop the mixed mode fracture criterion.

1.3 Research Objectives

The overall objective of this research is to understand and develop the mixed-mode fracture criterion of IM7-G/8552 Unidirectional Composite Laminate.

The Specific Objectives of the research are:

(a) Fabrication of IM7-G/8552 carbon/epoxy composite laminates.

(b) Determine interlaminar fracture toughness in mode I, mode II and mixed-mode I-II loadings.

(c) Finally develop Mixed-Mode Fracture criteria, G_C as a function of G_I and G_{II} loadings for IM7-G/8552 unidirectional composite laminate.

1.4 Scope of this Thesis

This thesis has been organized into six chapters. Chapter 1 presents the background of the research and literature pertaining to fracture modes and the ASTM testing methods (DCB, ENF and Mixed Mode testing). This chapter also includes research objectives, and the scope of the overall thesis. Chapter 2 describes the approach used to develop the Mixed-Mode (I-II) fracture criterion. A concise introduction followed by an explanation of Mode I, Mode II and Mixed-Mode I-II fracture toughness characterization methods. Finally, the data analysis, Mixed Mode fracture criteria and summary as also discussed. Chapter 3 presents the material properties of IM7-G/8552 and the specimen preparation procedures. Fabrication methods, specimen configuration and appropriate tables are provided and discussed for further elaboration. Chapter 4 provides an in-depth discussion of the testing and data analysis. Chapter 5 reports the results and discussion, relative charts, plots and tables are displayed. Finally, chapter 6 presents conclusions and future work recommendations.

CHAPTER 2

Approach to Develop Mixed-Mode (I-II) Fracture Criteria

2.1 Introduction

This chapter focuses on describing an approach to develop mixed mode (I-II) fracture criteria for IM7-G/8552 carbon/epoxy unidirectional laminate. The criteria is based on the hypothesis that fracture in a mixed mode loading is caused by both mode I and mode II loadings and the fracture energy release rate (G_C) can be expressed as,

$$G_C = G_{IC} + f\,(G_{II}^m) \qquad (2.1)$$

This and similar approaches have been used in this literature.

2.2 Approach

The development of mixed mode fracture criteria requires pure mode I and mode II fracture toughness and mixed mode fracture toughness for different mode I and II loadings. The figure 2.1 shows the steps used to develop mixed mode fracture equation. Throughout the thesis mixed-mode means the combination of mode I and mode II i.e. I-II.

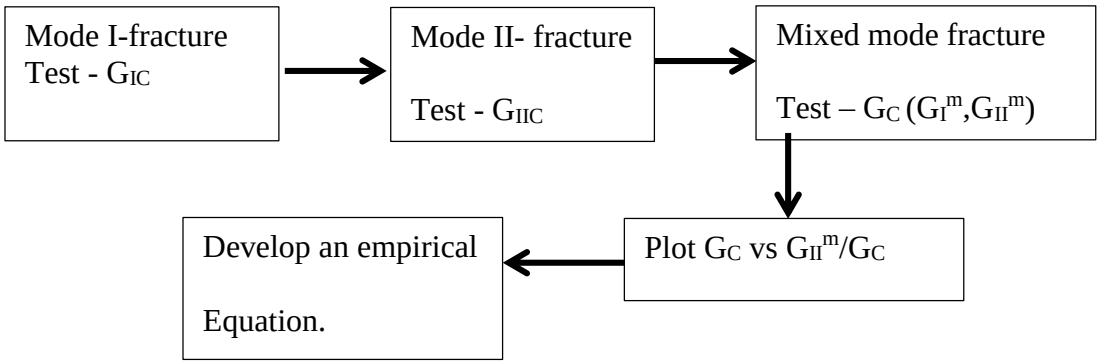

Figure 2.1: Methodology to develop mixed mode fracture criteria

Split (delaminated) beam specimen was tested by various loadings to generate mode I (G_{IC}), mode II (G_{IIC}) and mixed mode I-II (G_C) fracture toughness. Although this mixed mode fracture test apparatus [Crews & Reeder, Avva, Crews & Shivakumar, and ASTM Standard] can be used for all three types of tests but it is too crude for mode I and II fracture tests. Therefore, the standard double cantilever beam (DCB) and End Notched Flexure (ENF) were used to measure G_{IC} and G_{IIC}, respectively. The three test apparatus and loading used are shown in figure 2.2.

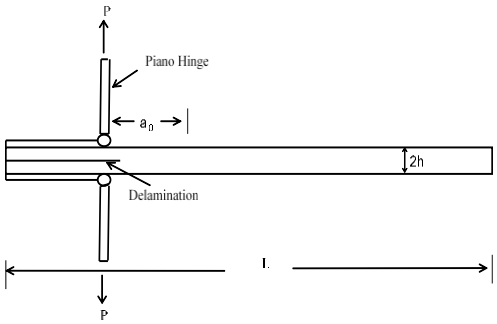

(a) Double cantilever beam test

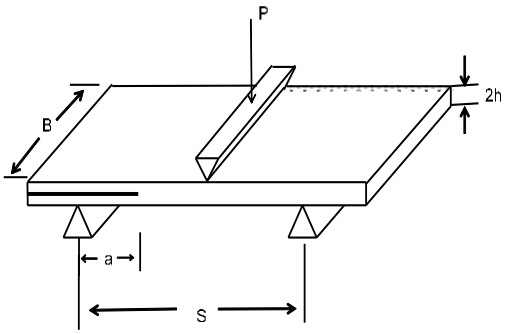

(b) End notched flexure test

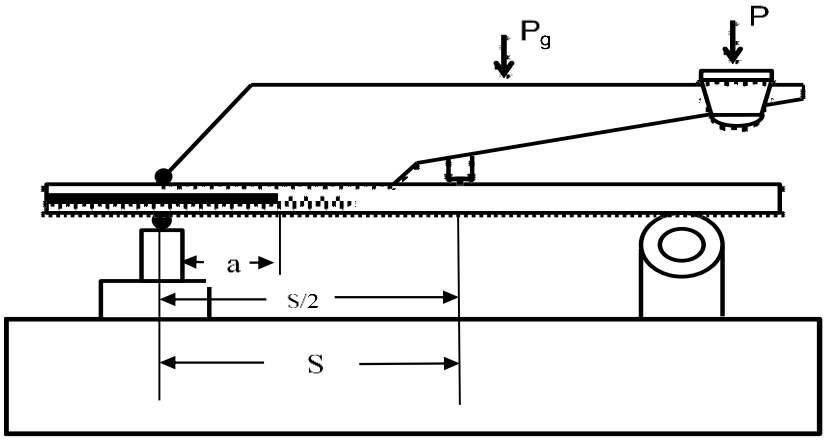

(c) Mixed-mode beam test apparatus

Figure 2.2: Three test apparatuses to measure pure mode I, II and mixed-mode fracture energy

release rates.

In figure 2.2, ‘a’ refers to delamination length, ‘B’ is specimen width, L is specimen length, and ‘S’ is span. In the figure 2.2 (c), P_g is the weight of the lever and P is the loading applied by a universal test frame. By moving the location of loading the combination of mode I (G_I^m) and II (G_{II}^m) are changed to cause fracture. Here G_I^m and G_{II}^m refer to mode I and mode II components of energy release rates, respectively. After measuring the fracture toughness for various loadings, the results are plotted as G_C against (G_{II}/G_C) (see fig 2.3). A smooth curve is fitted through the test data to provide a fracture equation represented by mode I and II loadings.

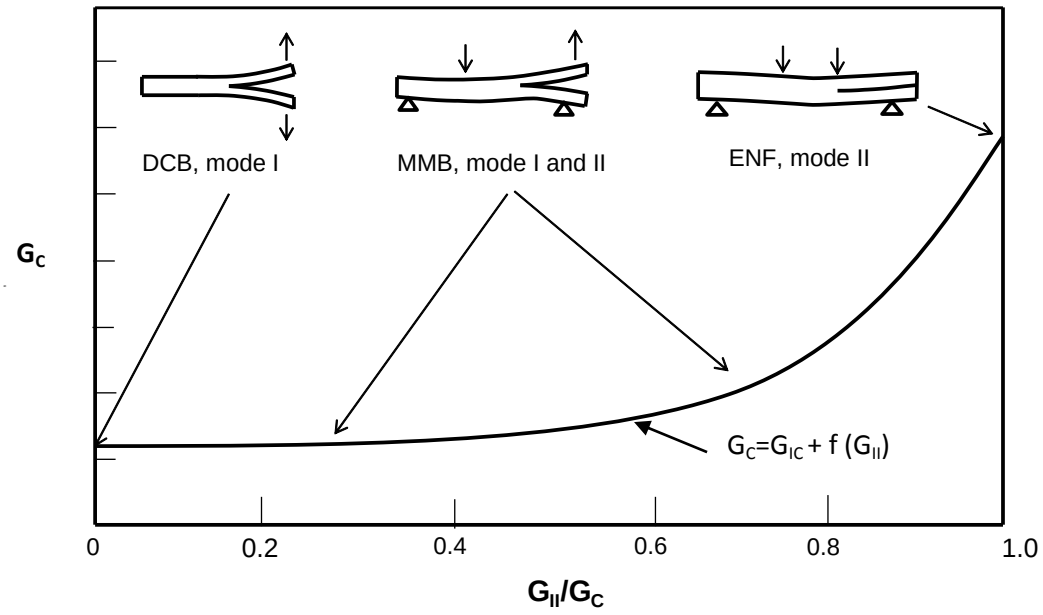

Figure 2.3: Typical mixed mode fracture data and empirical equation through the test data.

2.2.1 Mode I, $G_{IC,}$ of IM7-G/8552 Composite Laminate

The mode I test of IM7-G/8552 laminate was conducted by a former student of NC A&T [Ali, M., 2012.], according to ASTM standard D5528. The mode I test data was utilized in the development of mixed-mode fracture criterion.

Table 2.1 lists the values of G_{IC} calculated for five specimens. The average G_{IC} is 240 J/m^2 and the standard deviation of the data is 18 J/m^2. The coefficient of variation is 7.5%

Table 2.1: Mode I fracture toughness for IM7-G/8552 [Ali, M (2012)]

Type	Specimen #	2h, mm	B, mm	G_{IC}, J/m^2
DCB	1.1	3.40	25.50	248.7
	1.2	3.40	25.50	262.7
	1.3	3.40	25.50	225.9
	1.4	3.40	25.50	218.9
	1.5	3.40	25.50	243.4
	Average	**3.40**	**25.50**	**240**
	STD	**0.00**	**0.00**	**18**

2.3 Summary

Development of a mixed-mode fracture criteria and the associated test methods is presented in this chapter. A summary of mode I fracture toughness, G_{IC}, results are given. The average value of G_{IC} for IM7-G/8552 laminate is 240 J/m^2 and with a standard deviation of 18 J/m^2.

CHAPTER 3

Material and Specimen Preparation

3.1 Introduction

This chapter presents the fabrication of the laminates and specimen preparation for mode II and mixed mode I-II tests.

3.2 Material and Specifications

The material used for this fracture characterization is IM7-G/8552 unidirectional carbon fiber/epoxy laminate. Aerospace grade IM7-G/8552 prepreg material was manufactured and supplied by Hexcel Composites. The laminate and matrix properties are shown in tables 3.1 and 3.2, respectively. This material was selected for this study due to the usage in aerospace structures.

Table 3.1: 8552 Matrix Properties [Hexcel data sheet, 2013]

Property	**8552**
Tensile Strength (Mpa)	120.70
Tensile Modulous (Gpa)	4.67
Tensile Elongation (%)	1.70
Nominal Laminate Density (g/cm^3)	1.57
Fiber Density (g/cm^3)	1.79
Resin Density (g/cm^3)	1.30

Table 3.2: IM7-G/8552 Composite laminate's mechanical properties[Hexcel, 2013]

Property	
0° Tensile Strength (MPa)	2572
90° Tensile Strength (MPa)	174
0° Tensile Modulus (GPa)	163
90° Tensile Modulus (GPa)	10
In-Plane Shear Strength (MPa)	106

In the present research, aerospace grade IM7-G/8552 prepreg was chosen, supplied by Hexcel composites as rolls of prepreg tape of epoxy matrix (8552) reinforced with unidirectional carbon fibers (IM7-G). The roll measures 406.4 mm (16 in) in width, and it was stored in freezer at the manufacturer specified temperature of -23^0 C. The prepreg roll was stabilized to room temperature before being cut into 304.8 X 508 mm (12 X 20 inch) sized piles which are in a unidirectional orientation. The matrix and laminate properties are listed in tables 3.1 and 3.2, respectively. These results are referenced from the Hexcel product data sheet.

3.3 Fabrication of Panels and Test Specimens

Unidirectional IM7-G/8552 laminates were fabricated for mode II and mixed-mode (I-II) tests. There were two panels fabricated, each containing 24 plies, by following procedure specified by the material supplier. At the midplane of both laminate panels, a thin fluorinated ethylene propylene (FEP) film of 0.5 mil thick was introduced to serve as a starter crack for both the ENF (Non Pre-Crack) and the Mixed Mode (I-II) tests. Both Panels were fabricated at CCMR, the A&T Composite Manufacturing laboratory using the Autoclave process. The detailed fabrication procedure including prepreg cutting, stacking, debulking and molding are explained in the following sections.

3.3.1. Prepreg Cutting

The prepreg roll was taken out from the freezer and kept in room temperature overnight in order to stabilize. The roll was brought on to the cutting table where straight edges are fixed in a position in order to ensure straight consistent cuts for all prepreg sheets. A metal template was used to align the reference edge of the prepreg sheets with the straight edge. The dimensions of the metal rectangular template is 304.8 X 508 mm (12 X 20 inch). For each laminate, 24 sheets

of prepreg were cut. The process was duplicated for both Mode II and Mixed Mode (I-II) test laminates.

3.3.2. Stacking and Debulking

After cutting, the prepreg sheets are stacked together in pairs. After stacking, every two sheets of prepreg, debulking is carried out using a vacuum bag as shown in figure 3.2. The stacked plies are pressed against a straight reference straight edge, in order to eliminate ply deformation. For each debulking operation, the film is sealed and a vacuum of about 101.6 kPa was applied for 3 minutes. The precut FEP film is placed between the 12^{th} and 13^{th} plies in order to form a crack initiator. The 12^{th} and 13^{th} plies are chosen due to their location at the midplane of the laminate. These debulked and stacked prepregs are now ready for molding.

3.3.3. Molding

After debulking process, autoclave molding is carried out. The autoclave molding process consists of mold preparation, bagging and molding.

3.3.3.1. Preparation of Mold

The mold is nothing but a steel base plate with dimensions of 6.35 mm X 432 mm X 876 mm (0.25 in X 17 in X 34.5 in). The base plate was cleaned using isopropyl alcohol. A high temperature resistant flash tape is applied on the base plate. A double sided tape was applied on the mold on the perimeter of the metal template used for cutting the prepreg, leaving a gap of 12.7mm (0.5 in). A release film was applied on the mold and trimmed in such a way that it covers double sided tape which is the perimeter of the mold. Now a reference straight edge is used for which mold release was applied and flash tape was wrapped around it so that resin doesn’t stick to it. A double sided tape was applied on the top and bottom of the reference

straight edge and then the reference straight edge was aligned to the edge of the bottom release film which is on the base plate and placed firmly.

3.3.3.2. Bagging

Before placing the debulked prepreg on to the base plate the film on the base plate was cleaned in order to prevent the contamination of the prepreg during the process. Then the prepreg was placed firmly against the reference straight edge. A silicon rubber dam are tapped on the top and bottom with double sided tape, installed on three sides left around the debulk laminate. Over which breather string (7781 E-Glass) where placed on two edges and one in the middle of the laminate, as shown in figure 3.1. The TFE film was placed over the laminate and stuck to the tape on the rubber dam so that it cover the laminate from all the four sides.

Figure 3.1: Prepreg layup on the steel mold plate

Then the mold release was applied on top and bottom of the caul plate for two times and is then placed on the top of the film by making sure that it is aligned with the side of the reference straight edge and not to puncture the film. Pieces of flash tape are used to cover the gap if there are seen and seal it completely, which is in figure 3.2.

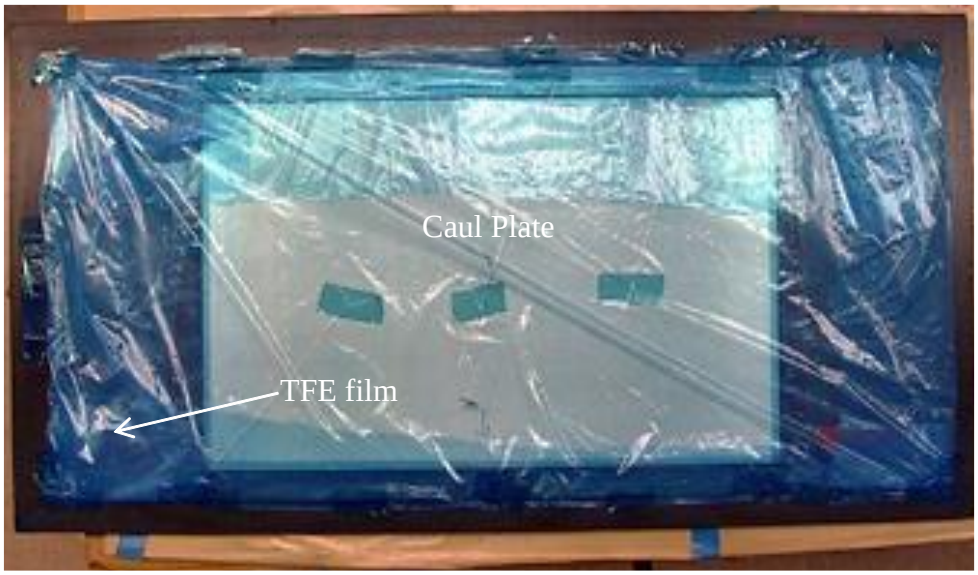

Figure 3.2: Caul plate covered with Wrightlon 5200B fluoropolymer release

Over the caul plate the air breather is placed so that it cover the cowl plate rubber dam and the reference straight edge and is taped with pieces of flash tape. Over the mold's vacuum port, a silicon rubber dam was installed with a double sided tape and a polyester breather was placed to cover the hole in the rubber dam. Double sided sealant tape was applied around the base plate and away from the mold and release film. A polyester breather of suitable size was cut and applied on the cowl plate and release film. The backing paper on the sealant tape was removed and polyester breather bag was gently tacked to the top of the exposed sealant tape and the extra polyester which was hanging was trimmed. After the bag is ready, it is tested for vacuum leak by closing the three-way valve from mold to vacuum pump, the vacuum leak rate

should not exceed more than 3.4 kPa/min. The figure 3.3 shows the molded panel that is ready for the autoclave curing process.

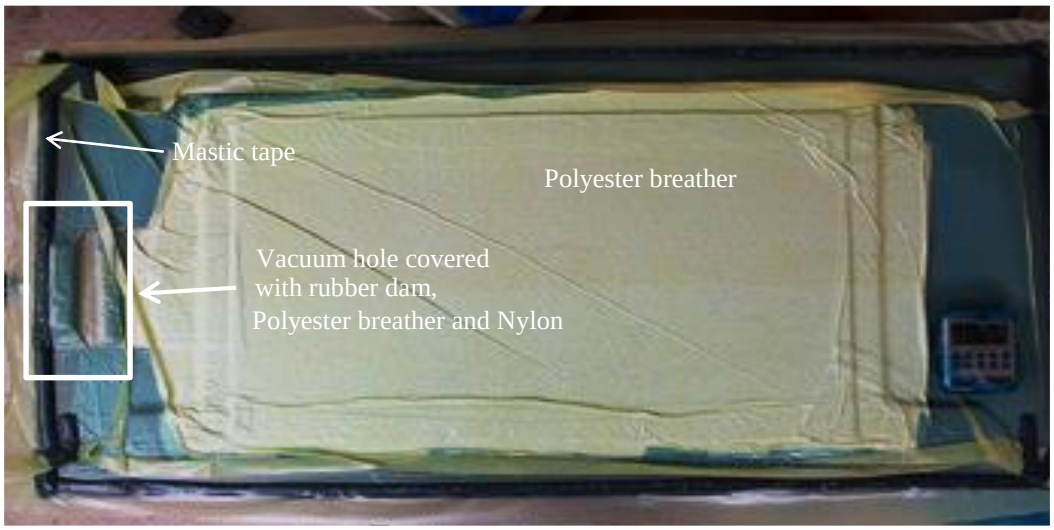

Figure 3.3: autoclave prepreg ready for procession

3.3.3.3. Molding

The completed vacuum bagged mold is inserted into the autoclave chamber, which is shown in figure 3.4 and the autoclave's vacuum line was attached to the mold's vacuum port.

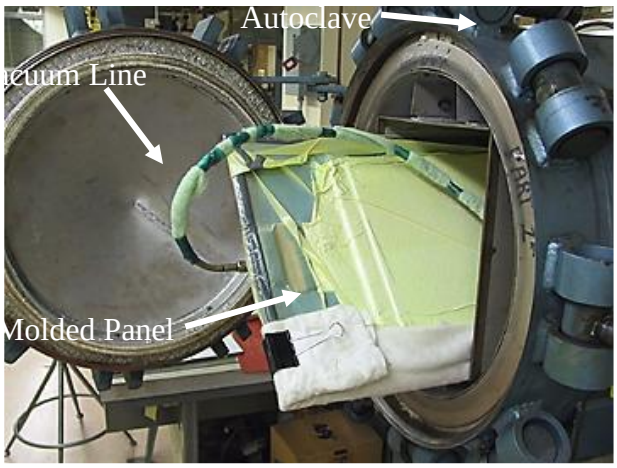

Figure 3.4: molded panel in the autoclave

The vacuum pump was turned on and tested for leaks again, once there are no leaks the autoclave door was closed and bolted. Appropriate curing cycle was initiated when nitrogen gas valves were opened and pressure was applied to the autoclave chamber. Resin viscosity rapidly decreased and resin chemical reaction started as the temperature shot up. At the temperature hold (180^0C), resin viscosity was minimum and applied pressure removes excess resin. To cure resin, the pressure was held at a constant 100 psi throughout the cure cycle. Then at the end of the cure cycle, the pressure is removed and the mold assembly was allowed to cool down to ambient temperature. The image of the autoclave molded laminate is shown in figure 3.5. Once the panel is made the laminate edges were trimmed and was visually inspected for any external damage.

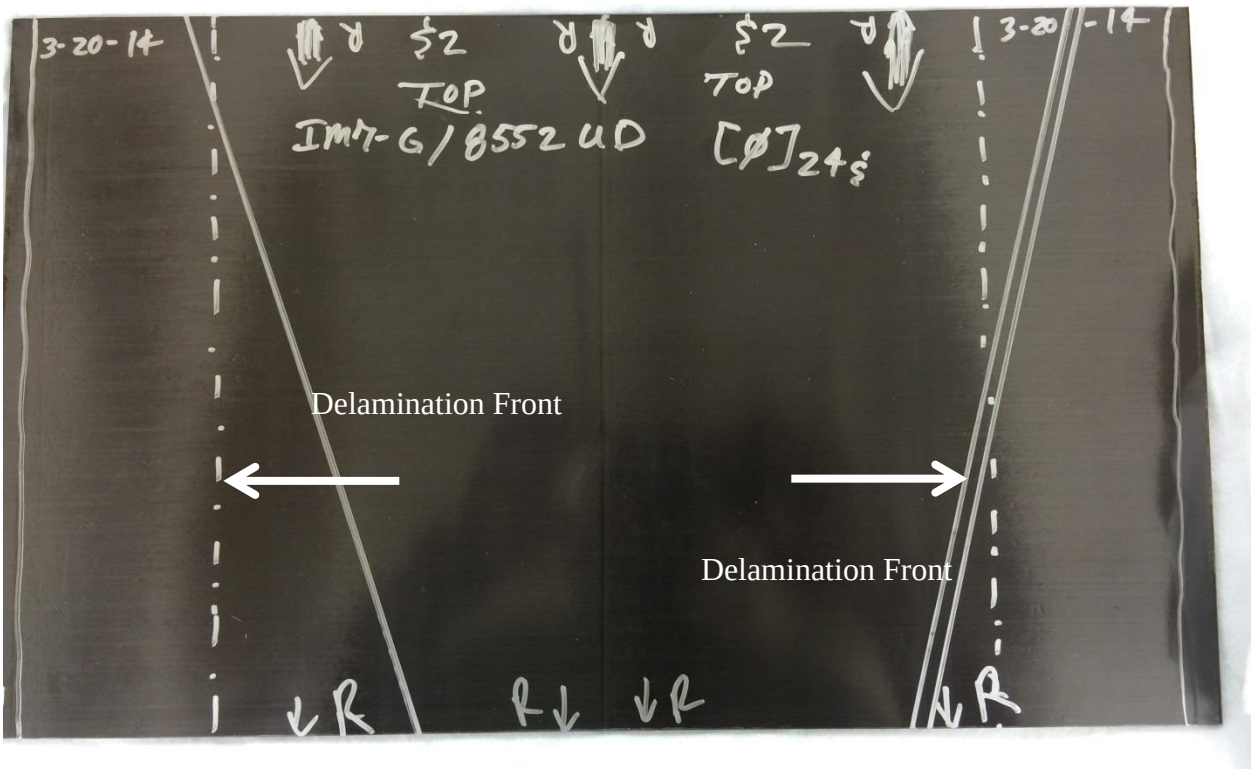

Figure 3.5: The IM7-G/8552 cured panel with delamination location.

3.4. Specimen preparation

Two laminate panels each measuring 304.8 X 508 mm (12 X 20 inches) are made, which are panel 1 and panel 2. Panel 1 was used for mixed-mode (I-II) testing and panel 2 was used for mode II testing. The specimen layout on panel # 1 is shown in figure 3.6. The sectional view is also shown in figure 3.6. The specimen id numbering scheme is indicated in figure 3.6. The first "XXX" is the test identifier, (ENF or IM7 for mixed mode), "X.X" refers to the panel and specimen numbers.

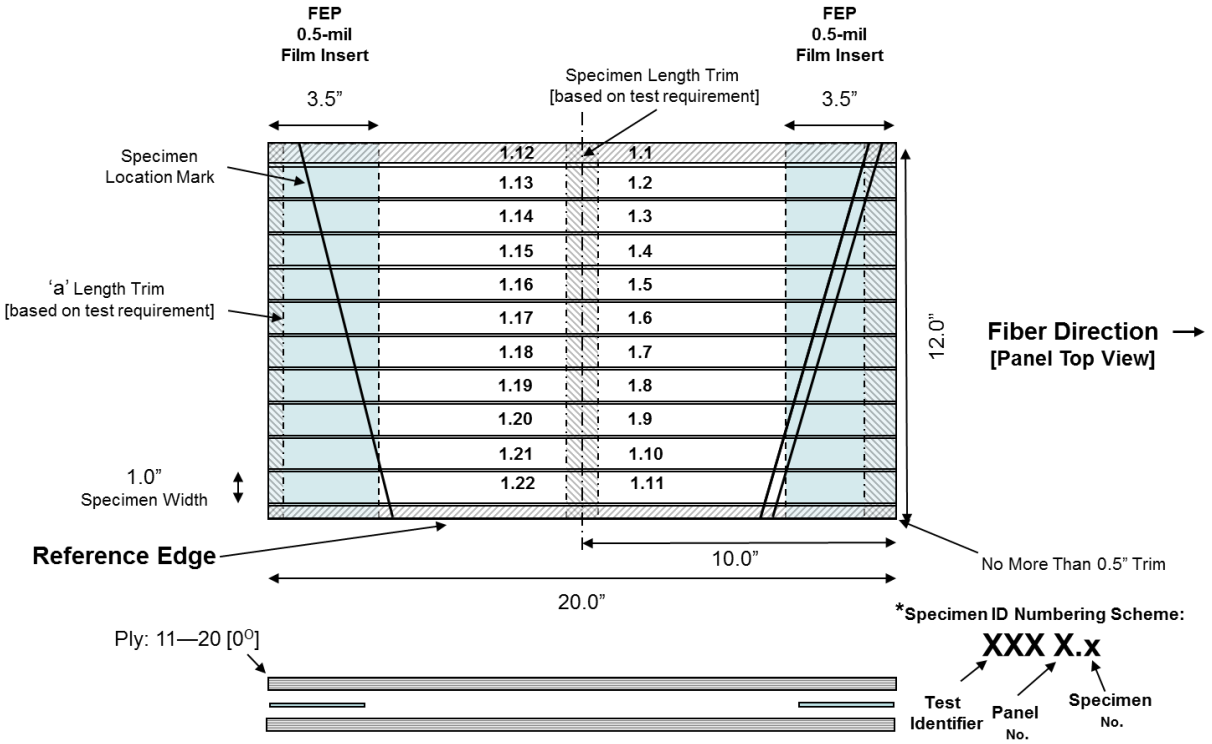

Figure 3.6: Specimen panel layout and specimen numbers

Each of the panel was cut on Chevalier saw using a diamond tipped cutting blade and lubricant is used to ensure dimensional accuracy, precision and to prevent early delamination. The figure 3.7, shows the specimen cutting operation.

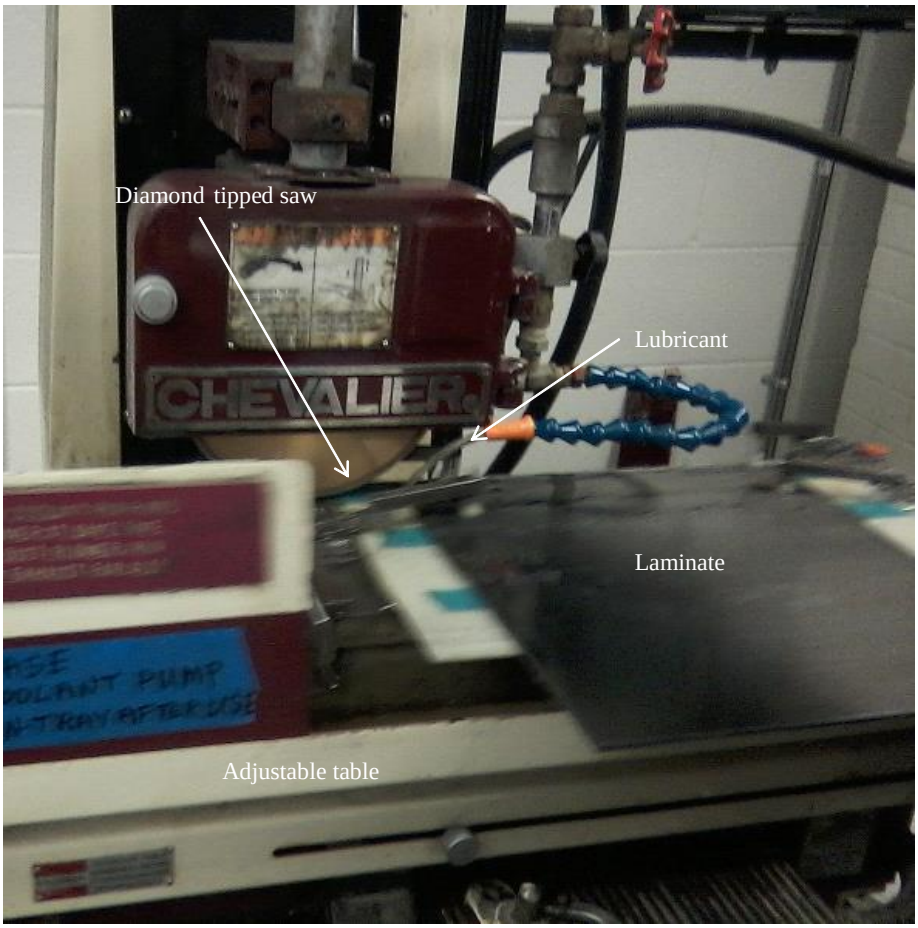

Figure 3.7: Specimen cutting operation

A reference edge on the panel was used for cutting the samples. Each panel contained twenty two (-22) specimens, only twenty (-20) of them were 25.4mm (1 in) and remaining two were extra (dummy) samples. The total number of specimens cut numbered 40, from which 20 specimens were used for mixed mode testing starting from IM7 1.1 to IM7 1. 20 from panel 1 and only five specimens were used for mode II, from panel 2. All the test specimens were of size

25.4 X 254 mm (1 X 10 in). Once the specimens were cut from the panel, they were taken onto grinding machine to grind the edges. The specimen dimensions were measured precisely using the Vernier caliper and are listed in table 3.3.

Table 3.3: Mode II and mixed Mode (I-II) Specimen Dimensions

Test	Specimen #	2h, mm	b, mm	Crack Length (a_0), mm	Length L, mm	E_{xx}, msi
Mode-II	ENF 2.1	3.67	25.48	25.40	177.80	*
	ENF 2.2	3.75	25.51	23.88	177.80	*
	ENF 2.3	3.78	25.43	23.62	180.98	*
	ENF 2.4	3.81	25.43	25.91	180.98	*
	ENF 2.5	3.84	25.48	24.64	180.98	*
Mixed Mode I-II (0.2)	IM7 1.1	3.81	25.40	25.76	152.40	17.89
	IM7 1.2	3.81	25.40	28.38	152.40	17.50
	IM7 1.3	3.81	25.43	27.24	152.40	19.38
	IM7 1.4	3.81	25.40	27.18	152.40	18.36
	IM7 1.5	3.81	25.40	25.84	152.40	18.28
Mixed Mode I-II	IM7 1.6	3.81	25.40	24.83	152.40	18.39
	IM7 1.7	3.81	25.40	25.91	152.40	17.35
	IM7 1.8	3.81	25.40	27.11	152.40	18.36
	IM7 1.9	3.81	25.65	26.92	152.40	16.63
	IM7 1.10	3.81	25.65	26.45	152.40	19.12
Mixed Mode I-II	IM7 1.22	3.81	25.40	26.46	152.40	17.69
	IM7 1.12	3.81	25.40	25.34	152.40	17.98
	IM7 1.13	3.81	25.40	27.22	152.40	17.88
	IM7 1.14	3.81	25.40	27.88	152.40	18.17
	IM7 1.15	3.81	25.40	26.57	152.40	18.62
Mixed Mode I-II	IM7 1.21	3.81	25.40	25.93	152.40	16.78
	IM7 1.17	3.81	25.40	25.86	152.40	17.84
	IM7 1.18	3.81	25.15	**	**	**
	IM7 1.19	3.81	25.15	25.55	152.40	17.78
	IM7 1.20	3.81	25.40	27.30	152.40	17.63

Flexural Modulus Not required for G_{IIc} calculations
** IM7 1.18 test failure: fixture contact**

After the specimens were prepared and edges were finished with fine sand paper. Then the finished test specimens were rinsed in distilled water and dried in an oven at 60°C for 24 hours. The geometries are then measured and recorded in table 3.3. The dried specimens are stored in a desiccator.

3.5 Summary

Two panels were fabricated, for mode II (ENF 2.1 – ENF 2.5) and mixed mode (I-II) testing (IM7 1.1 – IM7 1.20). The prepreg IM7-G/8552 was used with unidirectional 0° lay-up. Fabricated panels were visually inspected for defects and then cut into specimens and grinded to have a smooth finish on their edges. A total of 20 specimens were prepared for mixed-mode and 5 specimens for mode II testing.

CHAPTER 4

Testing and Test Data

4.1 Introduction

This chapter describes mode II and mixed-mode (I-II) testing and data analysis. The relevant results are presented in tables, figures and graphs. Mode I results were taken from the literature.

4.2 Mode II Fracture Test

The mode II fracture test was conducted using an End Notched Flexure (ENF) specimen with length, width and thickness of 152.4 mm, 25.4 mm and 3.8 mm, respectively. The specimen geometry and loading are shown in figure 4.1. Five specimens were tested using the ASTM draft 2012 standard for determining G_{IIc} of unidirectional laminates (ASTM-Draft Test Method, 2012). The test was carried out on a MTS load frame, similar to the equipment used during the Mode I fracture test. The 880 N (220 lbs.) load cell is used and the test was carried out under displacement control at a speed of 0.5 mm/min.

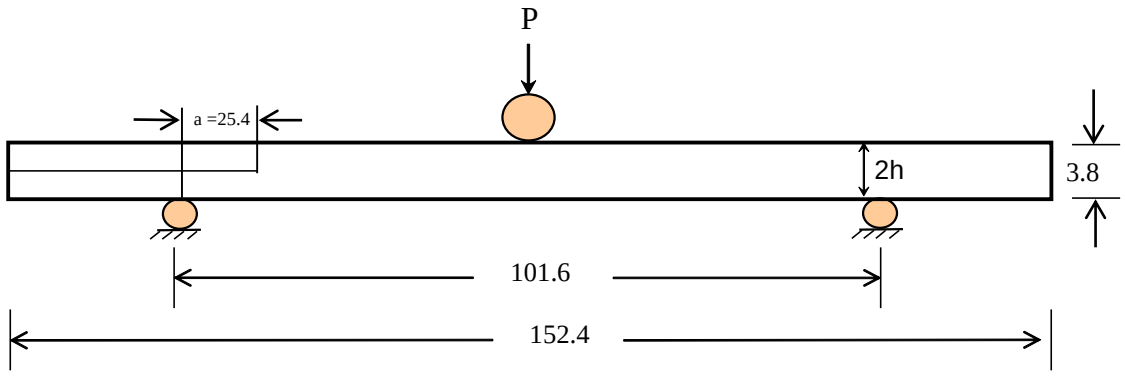

Figure 4.1: ENF test specimen and loading

4.2.1 Measurement of Delamination Tip

Before each test, the specimen was viewed under an optical microscope to locate the end of the Teflon film, which represents the location of the initial delamination tip. This location was marked with a carbide-tipped scriber on the edge of the specimen while viewing under the microscope. The procedure was repeated on the opposite edge. The mark was then seen under an illuminated magnifying glass while another scribe mark was made across the top of the specimen as the location of the crack front.

4.2.2 Testing

The specimen was then placed in a 3- point bend fixture (see fig 4.2) on a test machine with the span set for 101.6 mm as shown in figure 4.1. The specimen was placed in the test fixture in such a way that the scriber mark (indicating the delamination tip location) is 25.4 mm from the center of the left support roller. This positioning was done with the help of a precision steel scale and

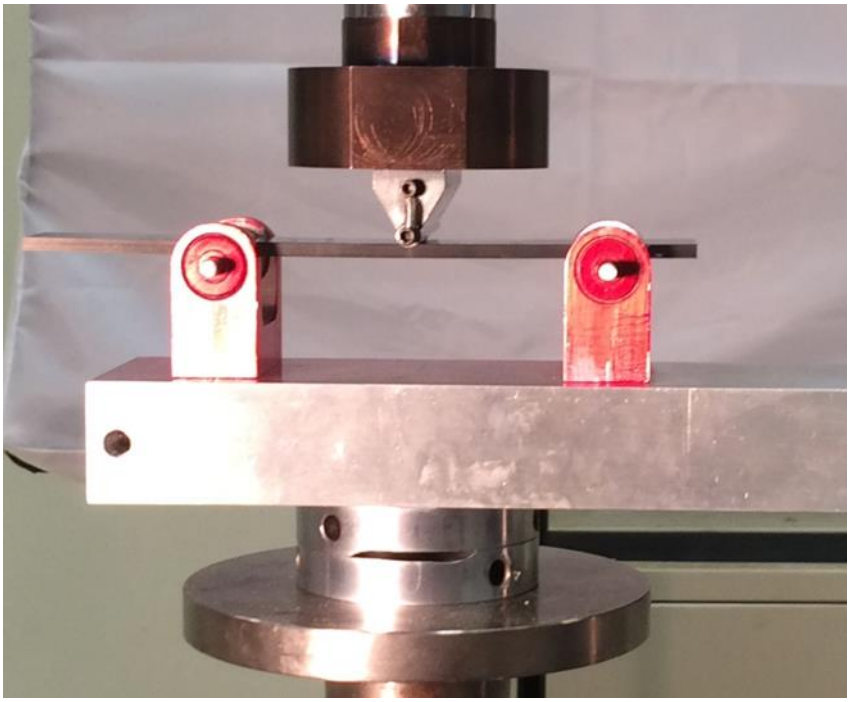

Figure 4.2: Test specimen and loading in a mode II fracture test

set the initial delamination length a_0 for the test to be 25.4 mm. The test was run at a displacement rate of 0.5 mm/minute while load and displacement data was acquired every 0.2 seconds. The test was stopped when the specimen fractures. The specimen fractured suddenly with a large drop in load indicating an unstable delamination growth. The figure 4.3 shows the load-displacement plot of five test specimens. The load-displacement data is shifted horizontally for better presentation. The load-displacement response is linear. It is observed from the figure for all the specimens. The failure load (P_C) and the slope (K) of the linear portion of the load-displacement graph are measured and listed in table 4.2. The compliance of the specimens was calculated by taking the inverse of the slope (K). The actual delamination length of the specimen was measured, after splitting the specimen into two halves. The lengths of delamination front at the two edges (left and right) and middle on these halves are then measured (see fig 4.4) and average value was recorded as a_i (delamination length) in the table 4.2.

4.2.3 Calculation of Mode II Toughness

The mode II fracture toughness (G_{IIC}) was calculated using the beam equation [Russell & Street, Daniel & Ishai 2005]. The calculated values of G_{IIC} for all specimens are listed in table 4.2.

$$G_{IIC} = 9\frac{(P_c a_i)^2}{2B}\left(\frac{C}{2L^3 + 3a_i{}^3}\right) \tag{4.1}$$

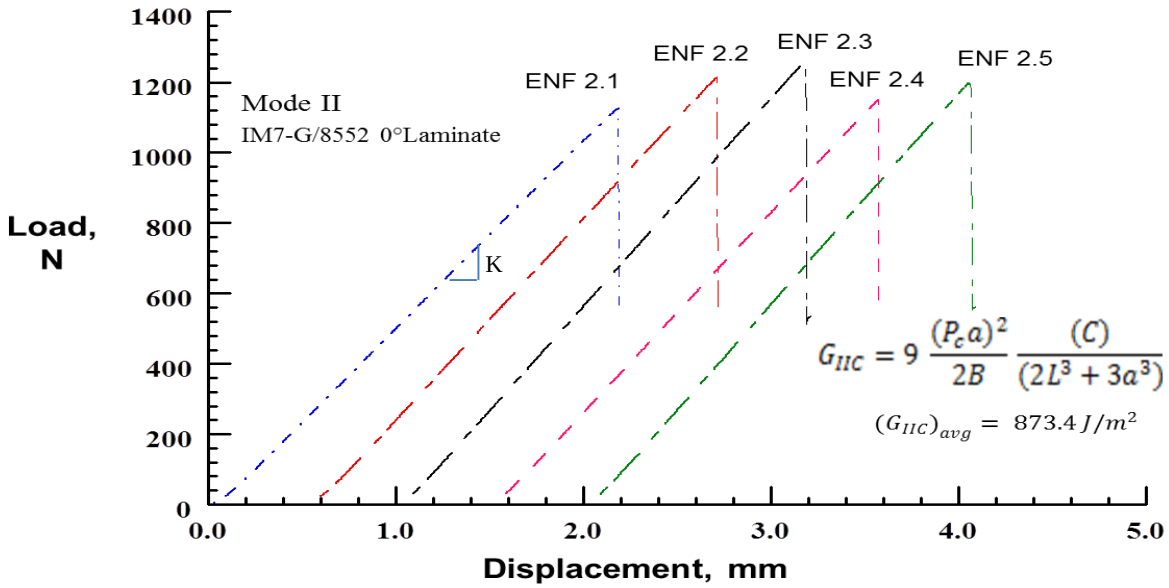

Figure 4.3: Load vs Displacement responses of mode-II tests specimens

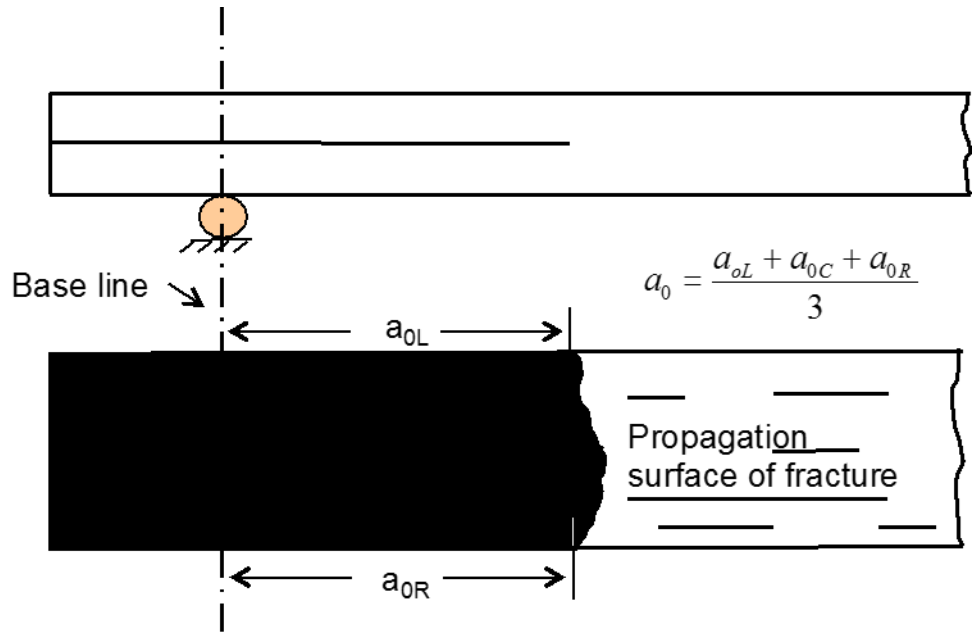

Figure 4.4: Delamination front location and measurement of average delamination length

Table 4.1: Mode II -No Pre Crack fracture test results (IM7-G/8552)

Sample #	Initial delamination length, a_o	Width, B	Pc	K	C=1/K	Delamination length, a_i	G_{IIc}
	mm	mm	N	N/mm	mm/N	mm	J/m^2
ENF 2.1	25.4	25.48	1126	510.43	1.96E-03	25.40	908.5
ENF 2.2	25.4	25.50	1044	432.71	2.31E-03	23.80	831.9
ENF 2.3	25.4	25.43	1102	454.32	2.20E-03	23.69	878.9
ENF 2.4	25.4	25.43	1150	545.84	1.83E-03	25.86	913.3
ENF 2.5	25.4	25.48	1179	578.79	1.73E-03	24.56	834.2
						Average	**873**
						STD	**39**

4.3 Mixed Mode (I-II) Fracture Test

4.3.1 Test Apparatus and Analysis

Mixed mode is a combination of mode I and mode II loading as explained in Crews & Reeder, Avva et al ., and the ASTM D6671-06 standard. The mixed mode bending (MMB) apparatus used in this study was developed by Avva et al., [Avva, crews & Shivakumar]. The schematic diagram of the test apparatus is shown in figure 4.5. The details of the analysis and calculation of mode I (G_I^m) and mode II (G_{II}^m) from the applied P and using the other specimen and loading arm parameters are presented in the above reference. The split beam specimen was a double cantilever beam specimen as explained for mode I testing. Then the specimen was loaded, by the compression load P. The load acting on the test apparatus and on the specimen are shown in figures 4.6a and 4.6b, respectively. The loading on the specimen (fig 4.6b) was resolved into

mode I and II components as in figures 4.6c and 4.6d, respectively.

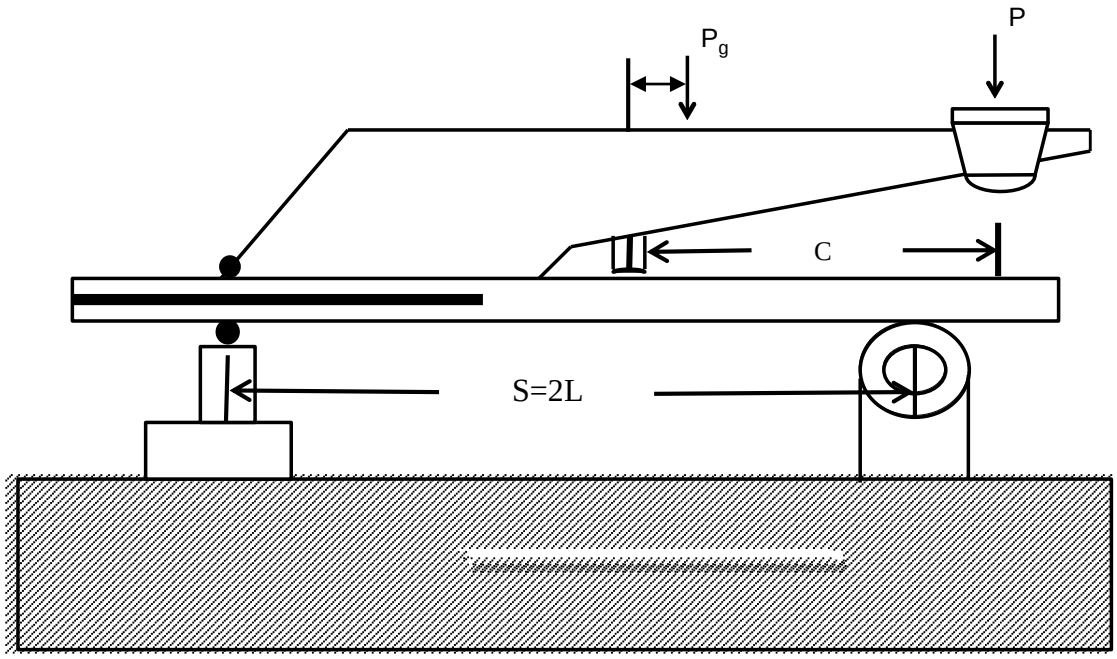

Figure 4.5 Schematic of the Mixed Mode test apparatus

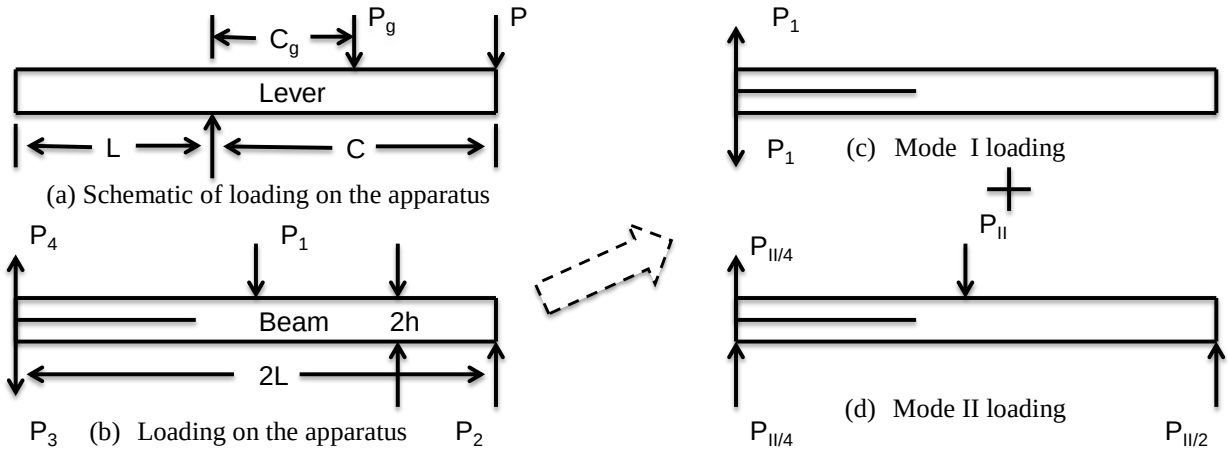

Figure 4.6: Loading on the test apparatus (a), test specimen (b) and resolution of loading into mode I (c) and mode II (d) loadings

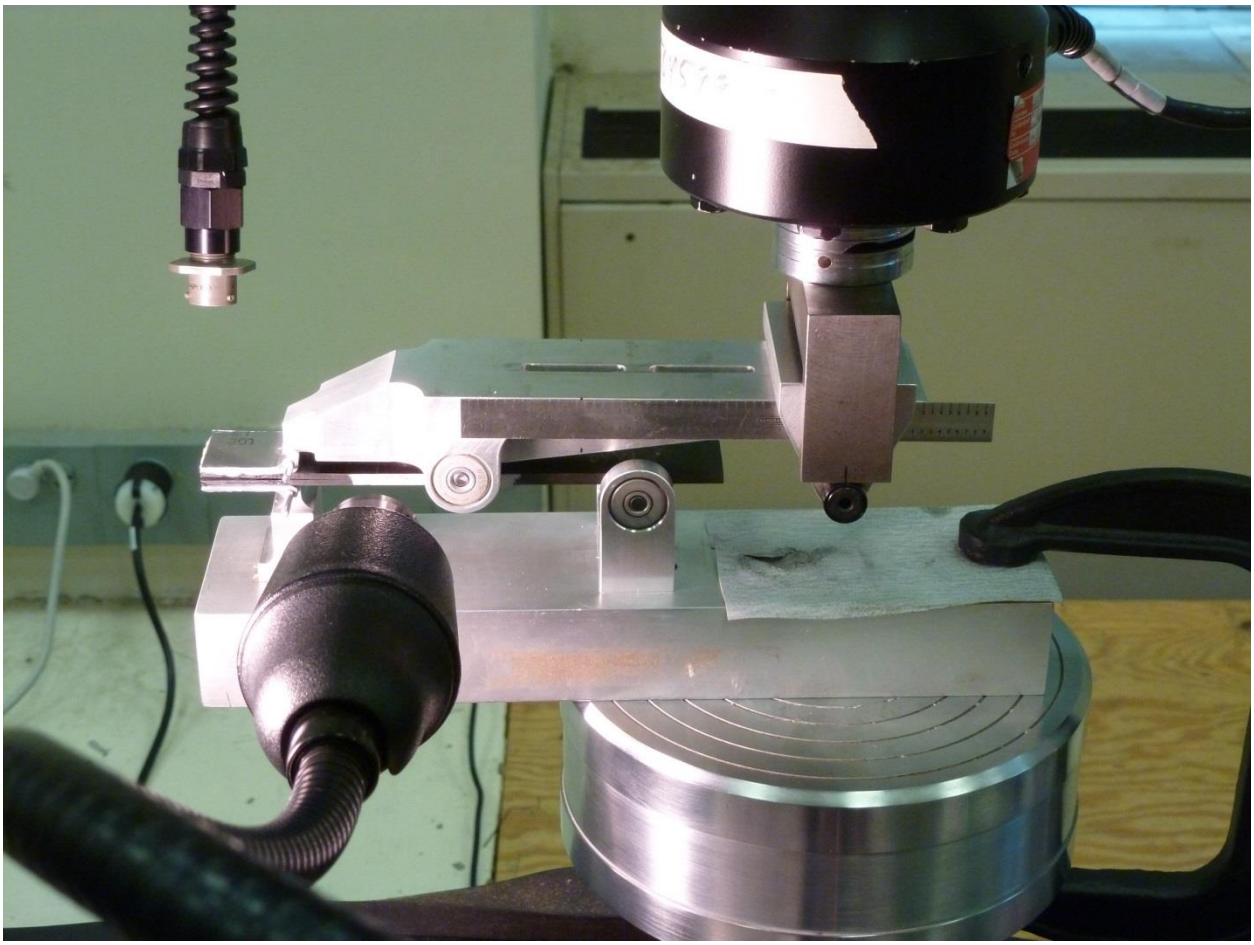

Figure 4.7: Actual Mixed Mode test apparatus

Here, the total load acting on the lever (P) is the sum of applied load (P_a) and the saddle weight (P_S).The lever weight is Pa, "2L" is the specimen span (S), and the parameters "c" and "c_g" are the distance from the specimen load point to the location of the load P and the center of gravity of the lever, respectively. Here, Pg = 0.754 lbs. (3.36N), P_S = 0.27 lbs. (1.2 N) and c_g = 1.35 in (34.3 mm).

The mode I loading is given by:

$$P_I = \left(\frac{3c - L}{4L}\right)P + \left[\frac{3c_g - L}{4L}\right]P_g \tag{4.2}$$

And the mode II loading is given by:

$$P_{II} = \left(\frac{c + L}{L}\right)P + \left[\frac{3c_g - L}{L}\right]P_g \tag{4.3}$$

The corresponding expressions for mode I and II strain energy release rate G_I^m and G_{II}^m are calculated using the values of P_I and P_{II} loading with their delamination length, moment of inertia and flexural modulus of the specimen. The expressions for G_I^m and G_{II}^m are given by:

$$G_I^{\ m} = \left(\frac{3P_I^{\ 2}}{BIE_{XX}}\right)\left(a^2 + \frac{2a}{\lambda} + \frac{1}{\lambda^2} + \frac{h^2 E_{XX}}{10G_{XZ}}\right) \tag{4.4}$$

$$G_{II}^{\ m} = \left(\frac{3P_{II}^{\ 2}}{64BIE_{xx}}\right)\left[a^2 + \frac{h^2 E_{XX}}{5G_{XZ}}\right] \tag{4.5}$$

Where λ is the elastic foundation constant given by

$$\lambda = \frac{1}{h}\sqrt[4]{\frac{6E_{ZZ}}{E_{XX}}} \tag{4.6}$$

Where, I is the moment of inertia of the beam ($I = \frac{1}{12}Bh^3$), the material properties E_{zz} and G_{XZ} were taken from the product data sheet [Hexcel 2013] and E_{ZZ} is 164 GPa and G_{XZ} is 106 MPa. The flexural modulus E_{XX} was measured for each specimen. The total energy release rate, $G_T = G_C$ is the sum of G_I^m and G_{II}^m at fracture.

4.3.2 Testing and Test Data

The location of the delamination tip was measured after the test as per the procedure explained in section 4.3. Before conducting the mixed mode fracture tests, four estimated values of G_{II}/G_T were selected, namely, 0.2, 0.4, 0.6, 0.8 assuming the lever is weightless. The calculated values of c for each of the G- ratios are listed in the table 4.4. Then, after moving the saddle to the require position, the specimen was tested in the MMB apparatus as shown in figure 4.7. The test fixture was preset for the specimen span (S) of 101.6 mm (4 in) and the initial delamination length of 25.4 mm (1 in). The saddle was moved on the lever to a precalculated value of c. The specimen was loaded under the displacement control at a rate of 0.5 mm/min. The failure was noticed by sudden drop in load. For low ratio of G_{II}/G_T, the delamination growth was stable and was able to monitor the crack propagation whereas for high values of G_{II}/G_T ($\geq$ 0.6), the fracture was brittle, the delamination propagated almost instantly to the mid span of the specimen.

The critical load for all four G_{II}/G_T and five specimens each are listed in table 4.4. Figure 4.9 through 4.12 shows the load-displacement responses for five specimens and the GII/GT values of 0.2, 0.4, 0.6 and 0.8, respectively. Notice the critical load increased with increased G_{II}/G_T value. As expected that P_C is smallest for mode I test and largest for mode II test.

After measuring the correct delamination length 'a_i' and measuring the flexural modulus E_{XX} (appendix), the mode I (G_I^m) and mode II (G_{II}^m) components and the mixed-mode fracture toughness (G_C) were calculated using equations 4.4 and 4.5, respectively. All the values of G_I^m, G_{II}^m and G_C are listed in table 4.5, as well as the recalculated values of G_{II}^m/G_C ratios.

Table 4.2: Estimated delamination length, (a_0), G_{II}/G_T ratio, measured delamination length (a_i), c values and critical load.

Estimated G_{II}/G_C	**Specimen #**	**Estimated Delamination Length a_0, mm**	**c, load position, mm**	**Critical Load, P_C, N**	**Delamination Length a_i, mm**
0.2	IM7 1.1	25.4	109.5	88.7	25.8
	IM7 1.2	25.4	109.5	82.8	28.4
	IM7 1.3	25.4	109.5	80.2	27.2
	IM7 1.4	25.4	109.5	89.6	27.2
	IM7 1.5	25.4	109.5	95.6	25.8
0.4	IM7 1.6	25.4	53.9	249.1	24.8
	IM7 1.7	25.4	53.9	233.3	25.9
	IM7 1.8	25.4	53.9	247.6	27.1
	IM7 1.9	25.4	53.9	226.6	26.9
	IM7 1.10	25.4	53.9	241.6	26.4
0.6	IM7 1.22	25.4	37.7	349.6	26.5
	IM7 1.12	25.4	37.7	431.7	25.3
	IM7 1.13	25.4	37.7	393.6	27.2
	IM7 1.14	25.4	37.7	384.7	27.9
	IM7 1.15	25.4	37.7	410.4	26.6
0.8	IM7 1.21	25.4	28.3	534.1	25.9
	IM7 1.17	25.4	28.3	635.6	25.9
	IM7 1.18*	25.4	28.3		
	IM7 1.19	25.4	28.3	617.2	25.6
	IM7 1.20	25.4	28.3	574.8	27.3

Table 4.3: Mixed mode (I-II) fracture toughness of IM7-G /8552 composite laminate

Estimated G_{II}/G_C	Specimen #	Crack Length a_i, mm	E_{xx}, † GPa	G_I^m, J/m^2	G_{II}^m, J/m^2	G_c, J/m^2	G_{II}^m/G_C
0.2	IM7 1.1	25.756	123.34	265.11	57.97	323.1	0.18
	IM7 1.2	28.385	120.67	254.93	55.52	310.5	0.18
	IM7 1.3	27.242	133.60	251.89	55.53	307.4	0.18
	IM7 1.4	27.178	126.59	274.55	60.29	334.8	0.18
	IM7 1.5	25.845	125.99	245.99	53.59	299.6	0.18
					Average	315	
					STD	14	CV= 4.4%
0.4	IM7 1.6	24.829	126.79	281.99	162.52	444.5	0.37
	IM7 1.7	25.908	119.59	318.94	184.70	503.6	0.37
	IM7 1.8	27.115	126.58	332.83	193.92	526.7	0.37
	IM7 1.9	26.924	114.66	322.16	185.97	508.1	0.37
	IM7 1.10	26.448	131.79	310.63	180.52	491.1	0.37
					Average	495	
					STD	31	CV = 6.2%
0.6	IM7 1.22	26.460	121.92	217.58	287.26	504.8	0.57
	IM7 1.12	25.337	123.92	269.96	355.58	625.5	0.57
	IM7 1.13	27.222	123.27	237.96	313.15	551.1	0.57
	IM7 1.14	27.877	125.25	232.99	306.45	539.4	0.57
	IM7 1.15	26.568	124.93	267.55	351.95	619.5	0.57
					Average	568	
					STD	53	CV = 9.73%
0.8	IM7 1.21	25.933	115.65	142.33	500.46	643.3	0.78
	IM7 1.17	25.864	122.97	133.54	468.07	601.6	0.78
	IM7 1.18*						
	IM7 1.19	25.552	122.56	165.92	585.94	751.9	0.78
	IM7 1.20	27.299	121.54	129.67	453.26	582.9	0.78
					Average	645	
					STD	76	CV = 11.78%

* Test Failure † See Appendix for Flexure Modulus

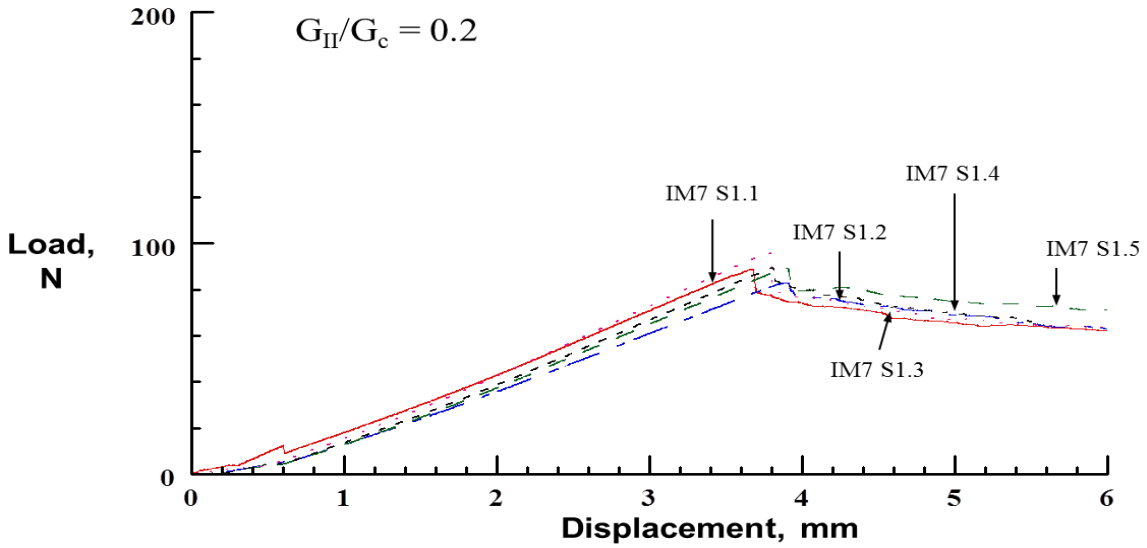

Figure 4.8: Load vs displacement for G_{II}/G_C =0.2 mixed mode (I-II) test specimens

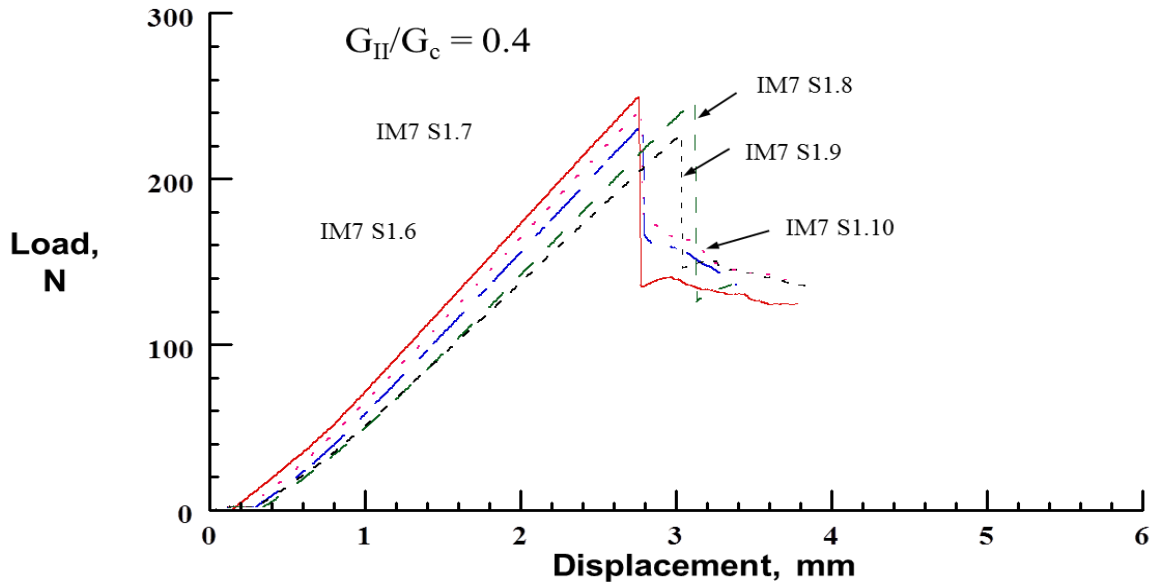

Figure 4.9: Load vs displacement response for G_{II}/G_C =0.4 mixed mode (I-II) test specimens

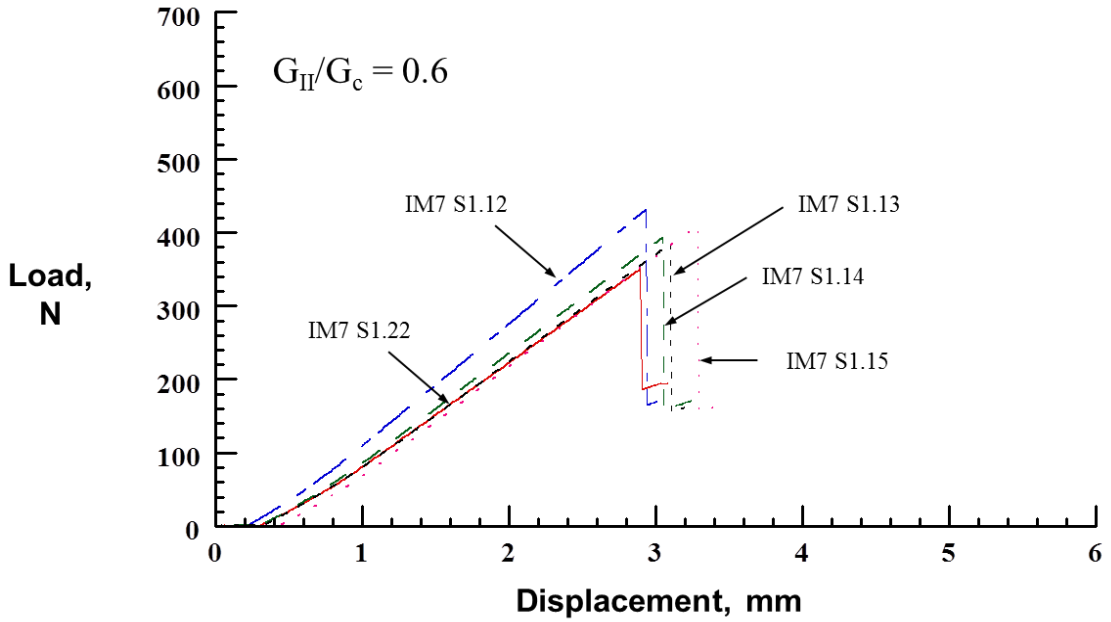

Figure 4.10: Load vs displacement response for G_{II}/G_C =0.6 mixed mode (I-II) test specimens

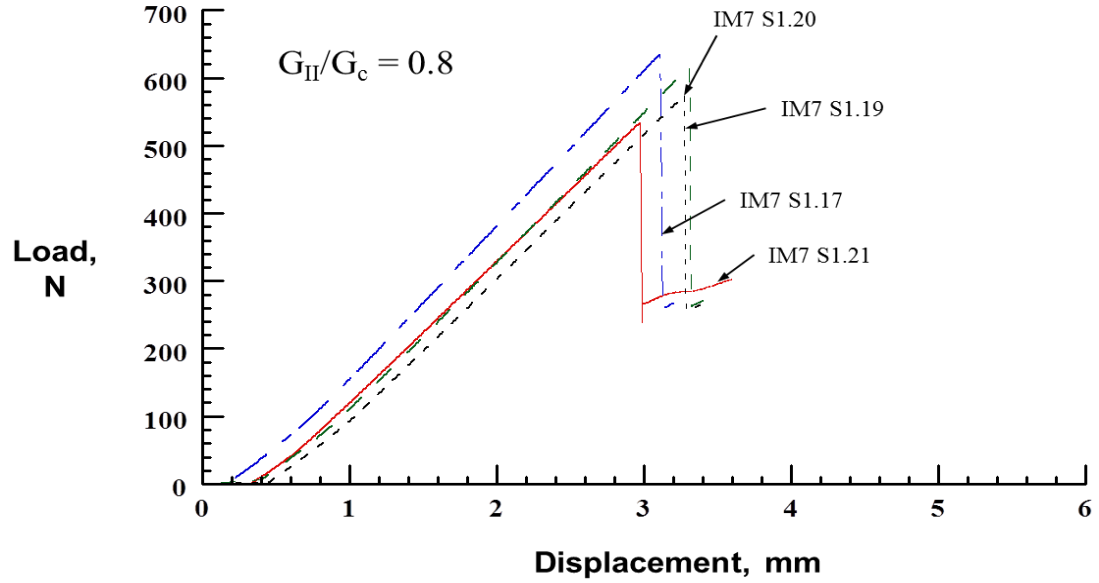

Figure 4.11: Load vs displacement response for G_{II}/G_C =0.8 mixed mode (I-II) test specimens

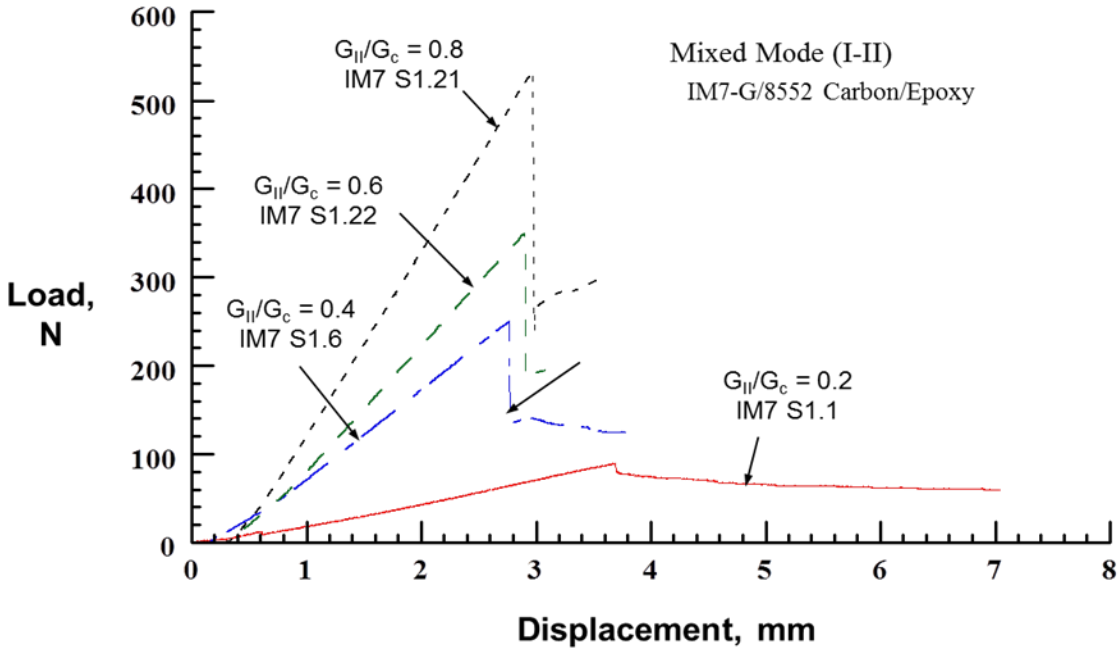

Figure 4.12: Load vs Displacement curve for various G_{II}/G_C values

4.4 Summary

The testing and data analysis procedures for mode II and mixed- mode at various G_{II}/G_T ratios is presented. Necessary equations essential to mode II and mixed-mode I-II energy release rate calculations are presented and discussed. A results summary of the average values of for G_{IC}, G_{IIC}, and G_C is presented in table 4.6.

Table 4.4 Summary of mixed-mode test results

Estimated, G_{II}/G_C	0.0	0.2	0.4	0.6	0.8	1.0
Actual G_{II}/G_C	0.0	0.18	0.37	0.57	0.78	1.0
Avg. G_C, J/m^2	240	315	495	568	645	873
STD	18	14	31	53	76	39

CHAPTER 5

Results and Discussion

5.1 Introduction

The summary of mode I, II and I-II data presented in the previous chapter are discussed in this chapter. From the data, a mixed-mode fracture criterion in the form of equation is developed. Both experimental and equation are compared with Hansen and Martins' results.

5.2 Mode I Fracture Test

The mode I fracture toughness of IM7-G/8552 laminate is taken from [5]. Table 2.1 summarizes the specimen dimensions and mode I fracture toughness values for IM7-G/8552 composite samples. The mode I fracture toughness, G_{IC}, of IM7-G/8552 laminate samples was in the range of 219 – 263 J/m^2. The average G_{IC} was around 240 J/m^2 with a standard deviation of 18.

5.3 Mode II Fracture Test

The load-displacement response of mode II (ENF) fracture tests for unidirectional IM7-G/8552 carbon/epoxy composites are shown in figure 4.4. Please note that the load-displacement curve of each specimen is shifted horizontally for better representation. From the figure it is observed that the load-displacement responses were nearly linear up to maximum load and then suddenly drops due to sudden fracture thereby indicating that the fracture is brittle. The initial slopes of the curves had little scatter which is an indication of good quality of the specimens. The slope of the initial portion of the load and displacement curve is measured for all specimens in order to compute compliance. The peak load, P_C, and compliance, C_0, are used in equation (4.1) to calculate energy release rate, G_{IIc}. Table 4.2 lists specimen width, peak load, compliance and computed energy release rate, G_{IIc} for all the IM7-G/8552 carbon/epoxy specimens. The average value of G_{IIc} is about 873.4 J/m^2 with a standard deviation (STD) of 39.1 J/m^2.

5.4 Mixed Mode (I-II) Fracture Test

The load-displacement response of mixed-mode (I-II) fracture tests for unidirectional IM7-G/8552 carbon/epoxy composites are shown in figures 4.8 through 4.11 for G_{II}/G_c = 0.2, 0.4, 0.6, and 0.8, respectively. From the figures 4.8 through 4.10 it is observed that the load-displacement responses (for G_{II}/G_c = 0.4, 0.6, and 0.8) were nearly linear up to maximum load and then suddenly drops due to sudden fracture. It is clear from the figure 4.11 that for G_{II}/G_c = 0.2, the load-displacement response was nearly linear up to maximum load and they become jagged, indicating the delamination growth. Only the mixed-mode test with G_{II}/G_c = 0.2 showed stable delamination growth. For comparison purpose, the typical load-displacement response of mixed-mode fracture tests with G_{II}/G_C ratios from 0.2 to 0.8 is plotted in figure 4.12. It is clear from the figure that the peak applied is increasing with increasing in G_{II}/G_c. Also it can be noted that the slope of the load-displacement graph is increasing with increasing value of G_{II}/G_c. The peak applied load, P_a, was used in Equations (4.4) and (4.25) to calculate delamination toughness of the material. Note that the total load P is the sum of the applied load P_a and saddle weight P_s. The values of the P_a are listed in Table 4.4. The computed fracture toughness of all the specimens is listed in Table 4.5. Average values of total energy release rate, G_c, at the initiation of delamination growth for G_{II}/G_c = 0.2, 0.4, 0.6, and 0.8 were 315, 495, 568, and 645 J/m^2, respectively. The standard deviation of the data ranged from 14 to 76 J/m^2.

Table 5.1: Summary of G_C for mixed mode (I-II)

G_C, J/m^2	G_{II}/G_c			
	0.18	0.37	0.57	0.78
Minimum	300	445	505	583
Maximum	335	527	626	752
Average	315	495	568	645
Standard Dev.	14	31	53	76

5.5 Mixed Mode (I-II) Fracture Criteria

Using the mode I, mode II and mixed-mode (I-II) mixed mode energy release rates for unidirectional IM7-G/8552 carbon/epoxy composite laminate, fracture criteria is developed for present work and compared with Hansen and Martins' fracture test results.

In figure 5.1, total energy release rate, G_c versus G_{II}/G_c is plotted based on the energy release rate data from mode I, mode II and mixed-mode fracture tests. For pure mode I test, G_c becomes G_{Ic} whereas for pure mode II test, the G_c becomes G_{IIc}. In figure the open symbol represent the individual specimen's data whereas the solid symbol represents the average of the five specimens' data. The figure clearly shows that the total energy release rate, G_c was increasing nonlinearly with increase in G_{II}/G_c. A quadratic equation was fit to the experimental data as shown in Figure 5.1 and it is given by

$$G = G_{IC} + 115\left(\frac{G_{II}}{G_c}\right) + 550\left(\frac{G_{II}}{G_c}\right)^2 \tag{5.1}$$

The equation agreed well with experimental data. Therefore, the fracture criterion for the IM7-G/8552 composite can be captured by simple form of the equation and is given by Equation (5.1).

Current results were compared with Hansen and Martins' mixed-mode fracture test results shown in table 5.2. Figure 5.2 shows the comparison of present fracture test data with Hansen

and Martins' test results. Large data scatter was observed in Hansen and Martins' fracture test data especially for G_{II}/G_C = 0.66 and 1 fracture tests. The coefficient of variation is high as about 29% and 22% for G_{II}/G_C = 0.66 and 1, respectively. The data scatter is within 12% for the present results which reflects the good quality of the test specimens fabricated in our lab. Only G_c of mode I and mixed mode test with G_{II}/G_C = 0.33 were in close agreement with the present fracture criteria equation whereas G_c of mixed mode test with G_{II}/G_C = 0.66 and mode II significantly deviate from the equation. From the figure 5.2 it is very clear that the G_c value reported by Hansen and Martin for the mode II test is significantly (~53%) higher than the present G_{IIc}. The present energy release rate was measured from standard 3-point bend ENF test whereas Hansen and Martin measured the energy release rate by 4-point bend ENF test. This perhaps the possible reason for significant deviation in the results. Also, it is noted from (Davies, 1999) that in 4-ENF tests, the measured energy release rate can be specimen geometry dependent and significantly (9-60%) higher than ENF results.

Table 5.2: Hansen and Martin fracture toughness for mode I, mode II and mixed-mode loading.[Hansen & Martin 1999]

	Mode I, G_{IC}	Mode II, G_{IIC}	Mixed Mode I-II, G_{II}/G_C	
			0.33	0.66
Avg G_C, J/m^2	208	1334	298	374
STD, J/m^2	9	293	42	109
CV %	4	22	14	29

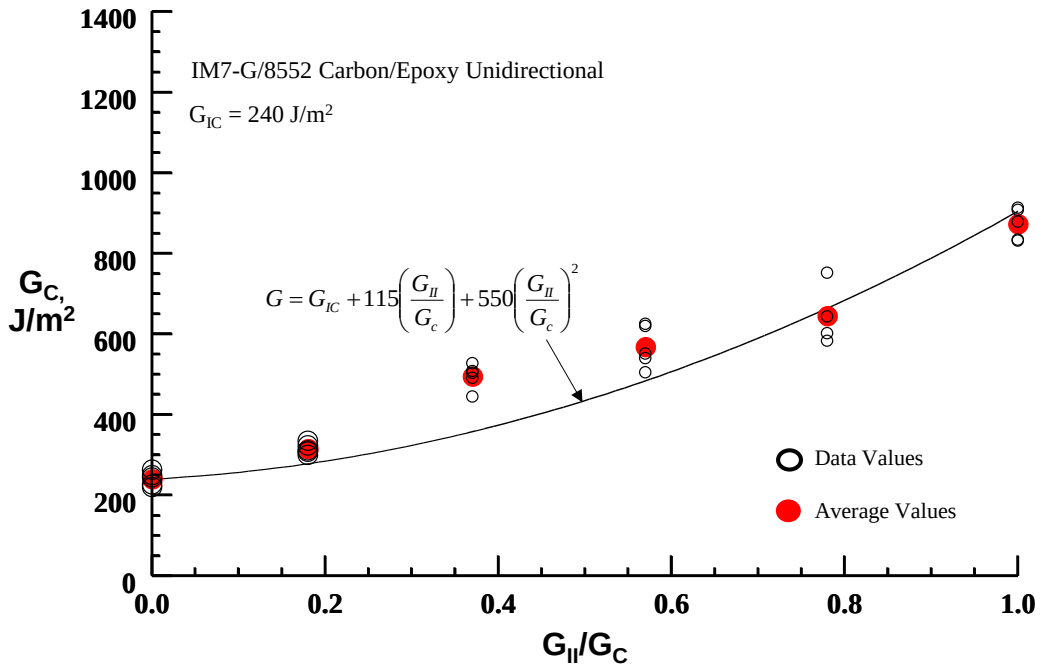

Figure 5.1: Mixed mode (I-II) fracture criteria for IM7-G/8552 composite laminates

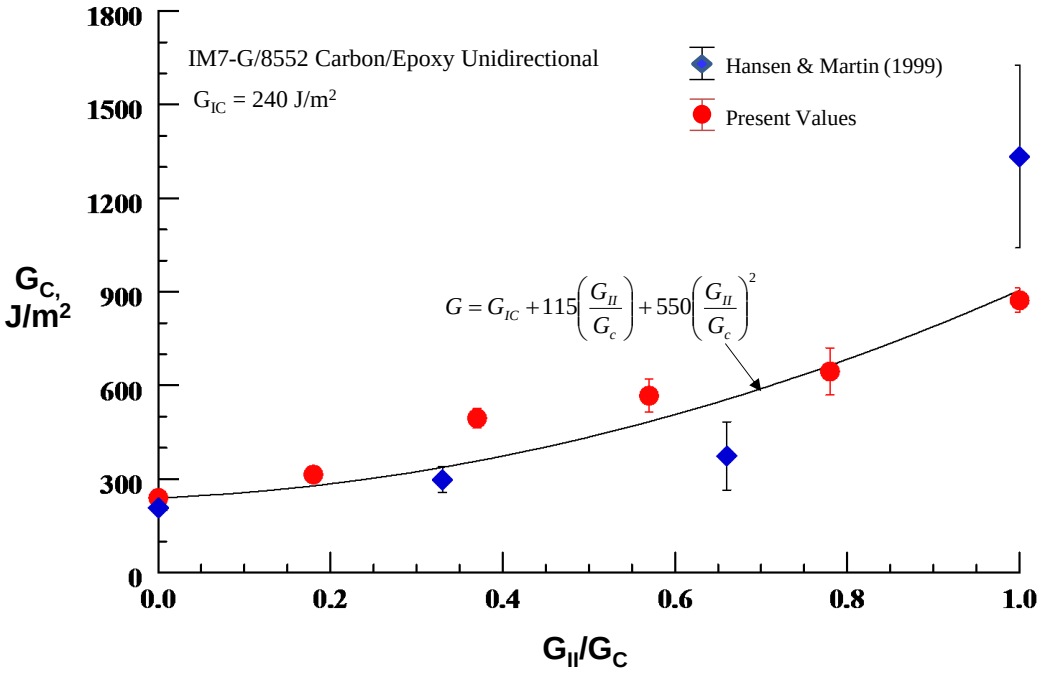

Figure 5.2: Mixed mode (I-II) fracture criteria for IM7-G/8552 composite laminates

5.6 Summary

Mode II and Mixed mode I-II fracture tests were conducted at G_{II}/G_C = 0.2, 0.4, 0.6 and 0.8. Mode I fracture tests data was taken from Ali's thesis, The average value of G_{IIc} is about 873.4 J/m^2 and the average values of total energy release rate, G_c, at the initiation of delamination growth for G_{II}/G_c = 0.2, 0.4, 0.6, and 0.8 were 315, 495, 568, and 645 J/m^2, respectively. A fracture criteria is developed for IM7-G/8552 carbon/epoxy composite laminate in the form of simple quadratic equation and compared with Hansen and Martins' mixed-mode fracture test results.

CHAPTER 6

Future Work and Conclusions

6.1 Conclusion

Majority of the Aerospace, including rotorcraft, structural components are subjected to bending and stretching loads that introduce peel and shear stresses between the composite plies. Delamination is a primary failure mode in composite laminates. Delaminations are caused by interlaminar stresses that act in the matrix layer, which is the weaker part of the composite laminate. Damage tolerant design of structures require two types of composite laminate data for the design of structures: 1. Mixed mode delamination criteria to predict failure and 2. Delamination growth rate to predict the life of a structural component. The focus of this research was primarily on the mixed mode fracture characterization of IM7-G/8552. Subsequently, composite panels were fabricated, specimens were prepared and tested under mode II and mixed mode loadings at G_{IIC}/G_C ratios of 0.2, 0.4, 0.6, and 0.8.

The equations, load and load-displacement curves for all the specimens are used to get a energy release rate for mode II and mixed-mode (I-II) loadings. The average value of G_{IIC} is about 873 J/m^2 with a standard deviation of 39 J/m^2. Mixed-mode tests were conducted for different estimated G_{IIC}/G_C ratios of 0.2, 0.4, 0.6, and 0.8, which gave value for G_I^m and G_{II}^m, whose summation is G_C. The average and standard deviation value of energy release rate, G_c, at the initiation of delamination growth for calculated G_{II}^m/G_c = 0.18, 0.37, 0.57, and 0.78 were 315 (14), 495 (31), 568 (53), and 645 (76) J/m^2, respectively. A fracture criteria is developed for IM7-G/8552 carbon/epoxy composite laminate in the form of simple quadratic equation given by

$$G = G_{IC} + 115\left(\frac{G_{II}}{G_c}\right) + 550\left(\frac{G_{II}}{G_c}\right)^2$$

The present values were compared with Hansen and Martin's fracture test results. The equation agreed well with the literature for G_{IC}, and $G_{II}^{m}/G_{C} = 0.33$ but it deviated for $G_{II}^{m}/G_{C} = 0.66$ and G_{IIC}. There is a significant (~53%) difference between the G_{IIC} values reported by Hansen and Martin and the present values and this can be attributed to the difference in mode II test methods. The present G_{IIC} values were obtained from a standard 3-point ENF test whereas the Hansen and Martin conducted a 4-point ENF test to compute G_{IIC}.

6.2 Recommendations and Future Work

Based on the result presented in this thesis, the following suggestions are made for future work:

- Study needs to be extended to other aerospace and rotorcraft materials
- Delamination growth rate under mixed mode stress state needs to be explored for this material

References

ASTM Standard 6671, (2006), Mixed Mode I-Mode II Interlaminar Fracture Toughness of Unidirectional Fiber Reinforced Polymer Matrix Composites, ASTM International, West Conshohocken, PA, 2006, D6671/D6671M-06, www.astm.org.

Adeyemi, N.B., Avva, V.S., Shivakumar, K.N. (1999) Delamination Fracture Toughness of Woven-Fabric Composites under Mixed-Mode Loading. AIAA Journal, 37 (4) 517-520

Adams, E. (2012). Mitigation of Delamination in Polymeric Composites by Polymer Nanofiber Interleaving. Unpublished doctoral dissertation, Mechanical Engineering Department, NC A&T State University: Greensboro, NC, USA

Akangah, P., Chen, H., Lingaiah,S., Russell Jr, L., Shivakumar,K., Swaminathan,G. (2009). Polymer Nanofabric Interleaved Composite Laminates. AIAA Journal 47(7), 1-18

Ali, M.A., (2012). Dissolvability of Polymer Nanofiber on Mechanical Properties of Interleaved Composite Laminates. Unpublished Master's Thesis, Mechanical Engineering Department, NC A&T State University: Greensboro, NC USA.

Ali. M., Chen, H., Shivakumar (2012), "Nanofiber Interleaved composites for Aerospace Applications," Journal of Aerospace Sciences and Technologies, Vol. 64, No. 1.

Ali, M., Miller, S., Panduranga,R., Sharper,M., Shivakumar, K,(2012) " Reactive Polyether Sulphone (r-PESU) Nanofiber Interleaved Composite Lmaniates," Proceeding of Sampe Tech 2012 CONF. North Charleston, South Carolina.

Arguelles, A., Bonhomme, J, Vina, J. (2009). Fractography and Failure mechanisms in static mode I and mode II delamination testing of unidirectional carbon reinforced composites. Polymer Testing 28 (612-617)

Arguelles, A., Bonhomme, J., Mollon, V., Vina, I., Vina, J. (2013). Influence of the Matrix

Toughness in Carbon Epoxy Composites Subjected to Delamination under Modes I, II and Mixed I/II, Mechanics of Advanced Materials and Structures, 20:8, 679-686, DOI: 10.1080/15376494.2012.667866

ASTM-Draft Test Method for Determination of the Mode-II Interlaminar Fracture Toughness of Unidirectional Fiber Reinforced Polymer Matrix Compsites, Date of Revision: June 28, 2013.

Avva, V.S., Crews Jr., J.H., Shivakumar, K.N., (1998). Modified Mixed-Mode Bending Test Apparatus for Measuring Delamination Fracture Toughness of Laminated Composites. Journal of Composite Materials, 32 (9) 1998

Benzeggagh, M.L. Kenane, M., (1996). Mixed-Mode Delamination Fracture Toughness of Unidirectional Glass/Epoxy composites under Fatigue loading. Composites Sciences & Technology 57 (1997) 597-605

Benzeggagh, M.L. Kenane, M., (1995). Measurement of Mixed-Mode Delamination Fracture Toughness of Unidirectional Glass/Epoxy Composites with Mixed-Mode Bending Apparatus. Composites Science & Technology 56 (1996) 439-449

Barikani, M., Saidpour, H.,et al. (2002) Mode I Interlaminar Fracture Toughness in Unidirectional Carbon-fiber/Epoxy composites. Iranian Polymer Journal/Vol. 11 No. 6

Czabaj, M.W., & Ratcliffe, J.G. (1998) Comparison of Intralaminar and Interlaminar Mode-I Fracture Toughness of Unidirectional IM7/8552 Graphite Epoxy Composite.

Daniel, I.M., & Ishai, O. (2005). Engineering Mechanics of Composite Materials. NY: Oxford University Press.

Davidson, B.D., Teller S., (2001) Recommendations for ASTM Standarized Test for Determining GIIc of Unidirectional Laminated Polymeric Matrix Composites. Journal of ASTM I. 7(2) Paper ID JAI102619

Davies P. (1999) Summary of results from the second VAMAS mode II round robin test exercise using the 4ENF specimen. IFREMER Report TMSI/RED/MS 99.82.

Hansen, P., Martin, R., (1999). DCB, 4ENF,MMB Delamination Characterization of S2/8552 and IM7/8552. US Army Technical Report, EROUSA

Karnati, S.,(2014). Mixed Mode Delamination fracture characterization of AS4/8552 unidirectional Carbon epoxy composite laminate. Unpublished master's thesis (NCATSU, CCMR)

Hexcel Corporation., (2013). HexPly 8552 Epoxy matrix product data, Hexcel Composites Publication FTA 072e

Martin R. H, Elms T, Bowron S. (1998) Characterization of mode II delamination using the 4ENF test. In: Proceedings of the 4th European Conference on Composites Testing & Standardization 1998, p. 161–70.

O'Brien, T., Johnson, W.M., Toland, G.J., (2010). Mode II Interlaminar Fracture Toughness and Fatigue Characterization of a Graphite Epoxy Composite Material. NASA/TM-2010-216838

Prasad, M. Jayaraju, T., Venkatesha, C., (2011). Experimental Methods of Determining Fracture Toughness of Fiber Reinforced Polymer Composites under Various Loading Conditions. Journal of Minerals & materials Characterization & Engineering, 10(13) 1263-1275

Appendix

Determination of Stiffness of Mixed Mode Tests Apparatus

The Appendix focuses on the measurement of the machine stiffness of the MTS load frame by conducting flexural tests on IM7-G/8552 composite specimens, using LVDT directly below specimen. Flexural test was conducted to measure the flexural modulus which is used for the computation of G_I and G_{II} in mixed mode fracture test.

The MTS load frame, along with the fixture are modeled as two springs connected in series as shown in Fig. A1

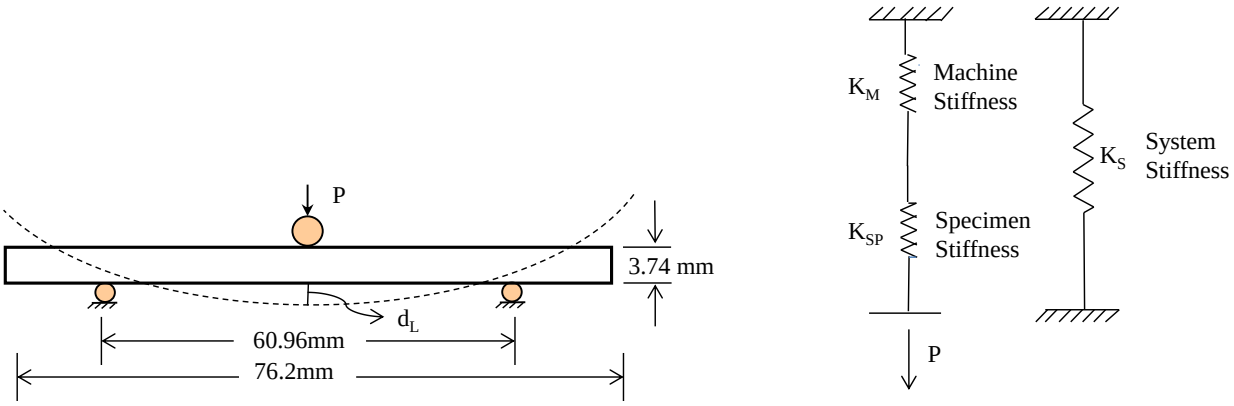

(a) (b)

Fig. A1. (a) Bending of the specimen during flexural test, (b) Model showing load frame and fixture as two springs connected in series.

The effective stiffness of the machine is given by Eq. (A1)

$$\frac{1}{K_S} = \frac{1}{K_M} + \frac{1}{K_{SP}} \tag{A1}$$

Where K_S is the stiffness measured based on machine displacement, K_M is machine stiffness and K_{SP} is specimen stiffness. A flexural test was conducted with LVDT placed directly below specimen at the load line. The schematic of specimen bending is shown in Fig. A1 (a).

K_{SP} is obtained by taking the initial slope of the load vs LVDT displacement (d_L) graph as shown in Fig.A2a. K_S is the initial slope of load vs machine displacement (d_M) graph as shown in Fig. A2b.

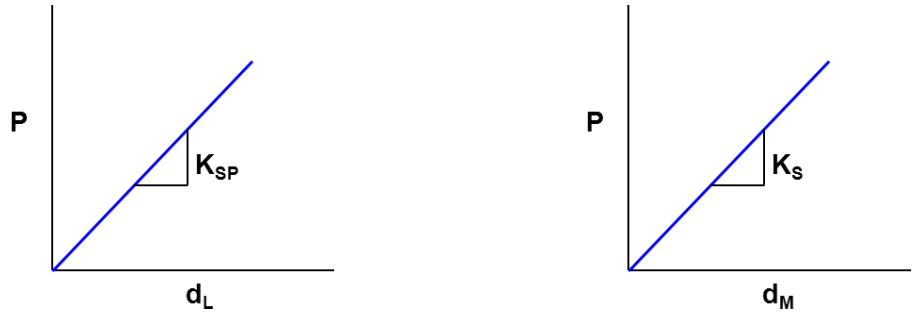

(a) (b)

Fig. A2. Determination of (a) specimen stiffness (K_{SP}) and (b) system stiffness (K_S)

Upon rearranging equation (A1), the equation for K_M is given by Eq. (A2)

$$\frac{1}{K_M} = \frac{1}{K_S} - \frac{1}{K_{SP}} \tag{A2}$$

The above equation is simplified and written as

$$K_M = \frac{K_{SP} K_S}{K_{SP} - K_S} \tag{A3}$$

The Stiffness K_S and K_{SP} were measured for several ENF specimens and KM is calculated from equation (A3). K_S, K_{SP} and K_M values are tabulated in Table A1.

The specimens used to conduct flexural test for calculating K_S and K_{SP} are extracted by cutting mixed mode tested specimen as shown in Fig. A3. The specimen dimensions used are 76.2mm long, 25.4 mm wide and 3.75 mm thick. The specimens used for flexural tests are IM7 S1.2, IM7 S1.3 and IM7 S1.4, initially the specimens were tested with the top layer of specimen facing the loading pin as shown in Fig. A4 (a) which is labeled as top in table and then specimen is flipped and tested again with the bottom layer facing the loading pin which is labeled bottom as in Fig. A4 (b).

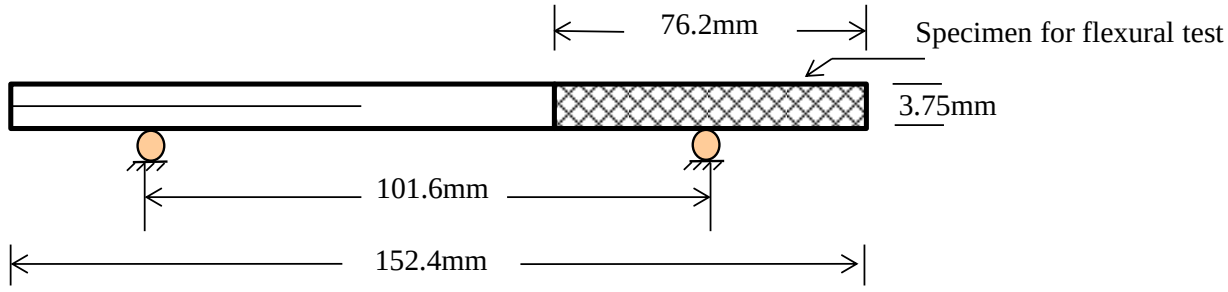

Fig. A3. Flexural Specimen extraction from ENF Test Specimen

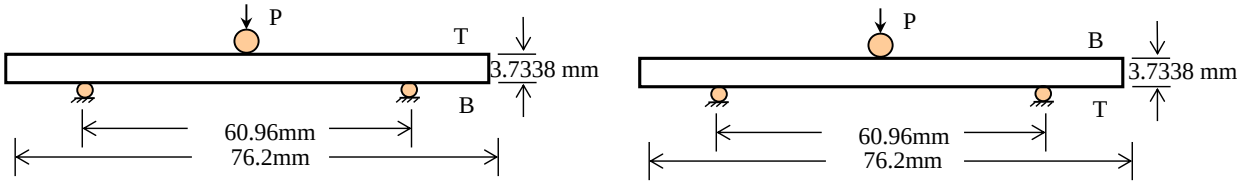

(a) (b)

Fig. A4. Flexural Test Specimen Configuration (a) Loading on top, (b) Flipped specimen test

Table A1. List of K_S, K_{SP} and K_M with average and standard deviation values.

Specimen #	**K_s, N/mm**	**K_{sp}, N/mm**	**K_m, N/mm**
IM7 1.2	2,923.3	3,146.4	41,236.0
IM7 1.3	2,957.9	3,186.5	41,236.1
IM7 1.4	2,984.6	3,217.5	41,236.0
Average	2955.3	3183.4	41236.0
STD	30.7	35.7	0.0

The average value of K_M obtained is 41,236 N/mm with a standard deviation of 0.0 which is 100.0%, of the average value. The K_M is much larger than K_{SP} and therefore the change in K_M will have a minimal impact on the specimen stiffness calculation.

Measuring Flexural Modulus Mixed Mode fracture Test specimens

Flexural test was conducted to measure the flexural modulus using the portion of Mixed Mode test specimens. The measured flexural modulus (E_{XX}) is used in the calculation of G_I and G_{II} in the mixed-mode fracture tests.

Flexural tests were performed according to ASTM D7264/D7264M. The tests were conducted using three-point bend fixture in MTS load frame. The flexural tests were conducted using the part of the mixed mode specimen which was cut from the mixed mode fracture tested specimen as shown in the figure A3. Five specimens were tested for each value of G_I/G_{II} ratios (0.2, 0.4, 0.6 and 0.8). The specimen length is 76.2mm, width is 25.4mm and 3.75mm thickness with a span of 60.96mm. All tests were conducted under displacement control at a constant

displacement rate of 0.5mm/min. The load and machine displacement were recorded and the stiffness (K_S) was calculated from the linear portion of the load-load line displacement graph. During the mixed mode test, the specimen IM7 1.18 had a metal contact that lead to crack extension beyond 76.2mm. Therefore, for these cases, the specimens were broken into two parts and tested separately. Thickness of these specimens were ‘h ’.

Figure A5 shows the plot of load versus machine displacement.

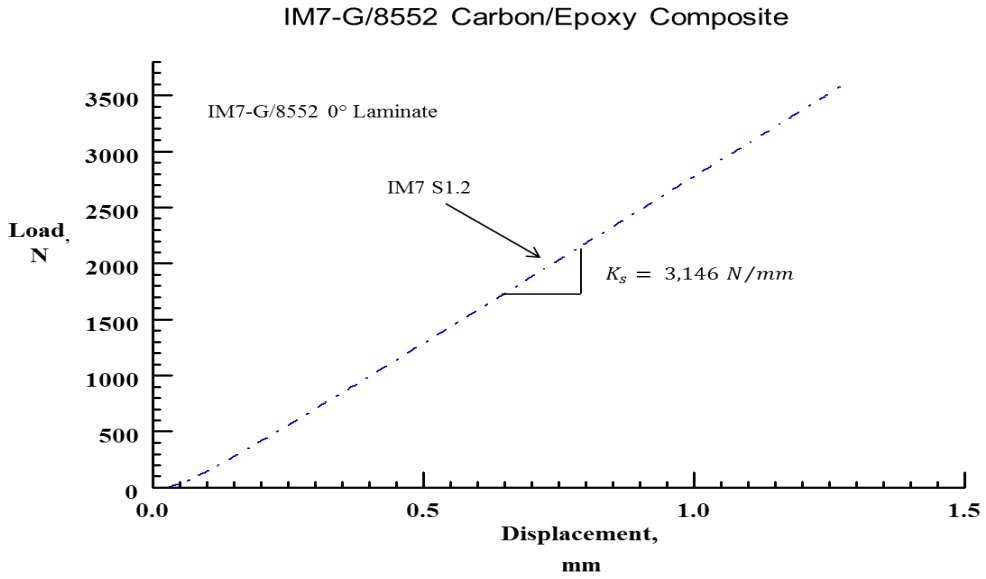

Fig. A5. Typical Load and machine Displacement response of IM7-G/8552 (IM7 1.2)

By knowing the value of K_M (=41,236 N/mm) and K_S, the specimen stiffness (K_{SP}) is calculated from equation given below

$$K_{SP} = \frac{K_M K_S}{K_M - K_S} \qquad \text{(A6)}$$

Using the value K_{SP} flexural modulus is calculated using the simply-supported beam equation Eq. (A7). Where L is span, b is width and t is thickness of specimen

$$E_{xx} = \left(\frac{K_{SP} L^3}{4bt^3} \right) \tag{A7}$$

Table. A2, A3 summarizes the calculation the flexural modulus (E_{XX}) which includes the values of specimen geometry b, t and K_{SP}, K_S. The average value of top and bottom test is listed in a separate column. The maximum flexural modulus value was 131.8 GPa and the minimum value is 114.7 GPa with an average value of 124.9 GPa and a standard deviation of 7.6. This shows the uniformity of specimen obtained from the same panel. This reflects the good quality of specimen. However the individual sample average is used for calculated G_I and G_I

Table A2: Determination of flexural modulus a mixed mode test specimen (IM7-G/8552)

Specimen #	2h, mm	b, mm	K_s, N/mm	K_{sp}, N/mm	K_m, N/mm	E_{xx}, GPa			Remarks
	Avg	Avg	Avg	Avg	Avg	T	B	Avg	
IM7 1.1	3.793	25.434	2,816.4	3,022.9	41,230.1	124.9	121.8	123.3	
IM7 1.2	3.869	25.489	2,923.3	3,146.4	41,236.0	120.8	120.6	120.7	
IM7 1.3	3.792	25.489	2,957.9	3,186.5	41,236.1	133.6	133.6	133.6	
IM7 1.4	3.835	25.510	2,984.6	3,217.5	41,236.0	126.4	126.8	126.6	
IM7 1.5	3.827	25.476	2,949.6	3,176.8	41,234.5	126.8	125.2	126.0	
IM7 1.6	3.852	25.519	3,026.6	3,266.4	41,236.0	126.6	127.0	126.8	
IM7 1.7	3.869	25.510	2,901.2	3,120.7	41,235.0	120.2	119.0	119.6	
IM7 1.8	3.852	25.442	3,013.6	3,251.2	41,235.8	126.9	126.2	126.6	
IM7 1.9	3.861	25.561	2,777.8	2,978.4	41,232.9	113.6	115.7	114.7	
IM7 1.10	3.827	25.527	3,080.8	3,329.6	41,235.5	132.3	131.3	131.8	
IM7 1.22	3.768	25.485	2,739.6	2,934.6	41,236.0	122.1	121.7	121.9	†
IM7 1.12	3.903	25.493	3,070.2	3,317.2	41,236.0	124.0	123.8	123.9	
IM7 1.13	3.844	25.493	2,927.9	3,151.6	41,235.9	123.5	123.0	123.3	
IM7 1.14	3.793	25.468	2,860.7	3,073.9	41,235.9	125.0	125.5	125.3	
IM7 1.15	3.751	25.442	2,833.6	3,042.6	41,235.7	128.7	128.0	128.3	
IM7 1.21	3.869	25.434	2,804.1	3,008.9	41,214.9	112.9	118.4	115.7	†
IM7 1.17	3.869	25.455	2,971.1	3,201.9	41,216.8	120.2	125.7	123.0	
IM7 1.18	3.945	25.451	3,155.0	3,416.4	41,235.7	124.1	123.4	123.8	
IM7 1.19	3.962	25.442	3,162.9	3,425.6	41,233.9	123.5	121.6	122.6	
IM7 1.20	3.878	25.485	2,960.3	3,189.3	41,220.2	124.0	119.1	121.5	
Average								124.9	
STD								7.6	

† IM7 1.11 Test failure, † IM7 1.16 Test Failure: